Clique Homology is QMA_1-hard

Supplementary Material

Marcos Crichigno[(1)] and Tamara Kohler[(2)]

[(1)] Blackett Laboratory, Imperial College London

[(2)] Instituto de Ciencias Matemáticas, Madrid

crichigno@proton.me, tamara.kohler@icmat.es

In this Supplementary Material we present the technical details and the proofs of the results presented in the main text. The material is split into Supplementary Methods and Supplementary Discussion. The Supplementary Methods are structured as follows. In Section 1.1 we give a review of basic elements of simplicial complexes and homology. In Section 1.2 we give our definition of the class QMA_1 and review Bravyi's clock construction showing QMA_1-hardness of quantum k-SAT. In Section 1.3 we present the proof that clique homology is QMA_1-hard, the main result in the paper. In the same section we also show that a version of the homology problem with a suitable promise is contained in QMA. In the Supplementary Discussion we discuss the relation of our results to supersymmetric quantum mechanics.

Contents

Chapter 1

Supplementary Methods

1.1 Review of Simplicial Homology

We begin by giving a review of basic elements of simplicial homology and the clique/independence complex. Readers familiar with this may skip this section.

1.1.1 Simplicial Homology

Simplices are the basic building blocks of simplicial complexes. A 0-simplex is a point, a 1-simplex is a line, a 2-simplex is a triangle with its face included, a 3-simplex a solid tetrahedron, etc. Consider a set of $(n+1)$ vertices $V = \{x_0, x_1, \cdots, x_n\}$. A p-simplex corresponds to a subset of these vertices with $p+1$ elements and is denoted

$$\sigma^{(p)} = [x_0 \cdots x_p]\,. \tag{1.1.1}$$

We will consider always an ordered set V, which leads to oriented simplices. The orientation of a p-simplex is determined by the ordering of its vertices. An oriented 1-simplex $[x_0 x_1]$, for instance, is a directed line segment in the direction $x_0 \to x_1$. The orientation of a 2-simplex $[x_0 x_1 x_2]$ is similarly induced by the ordering of its vertices, and similarly for higher dimensional simplices (see Fig. 1.1). Permuting the vertices leads to an equivalent simplex, possibly up to an overall sign indicating whether the simplex has a positive or negative orientation. Precisely,

$$[x_{i_0} x_{i_2} \cdots x_{i_p}] = \mathrm{sgn}(P)\,[x_0 x_1 \cdots x_p]\,, \tag{1.1.2}$$

where $\mathrm{sgn}(P)$ is the parity of the permutation from $\{01\cdots p\}$ to $\{i_0 i_2 \cdots i_p\}$. Taking a $(q+1)$-subset of the

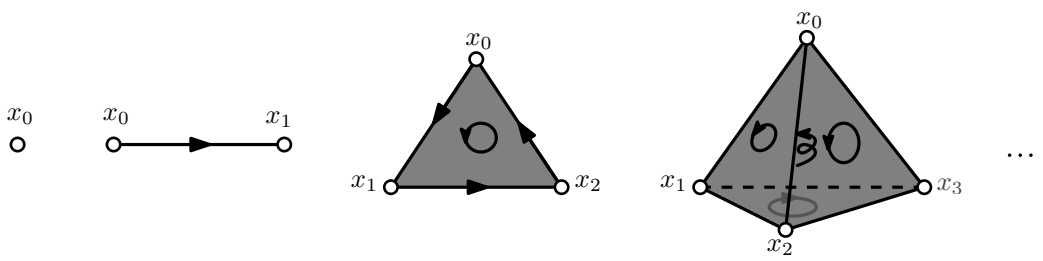

Figure 1.1: Geometric representation of a 0-simplex, oriented 1-simplex, oriented 2-simplex, etc.

vertices of a p-simplex defines a q-simplex called a q-face and denoted $\sigma^{(q)} \leq \sigma^{(p)}$. Similarly, one says that $\sigma^{(p)}$ is a coface of $\sigma^{(q)}$.
An (abstract) simplicial complex K is a set of simplices satisfying two requirements:

1. If a simplex is in K, then all of its faces are also in K and;
2. The intersection of any two simplices in K is a face of each of them.

The first condition states that a simplicial complex must be a set which is closed under taking subsets. For instance, a simplicial complex corresponding to a filled in triangle is given by the set $K = \{[x_0], [x_1], [x_2], [x_0x_1], [x_1x_2], [x_2x_0], [x_0, x_1, x_2]\}$. The second condition indicates how simplices can be "glued" to each other implying, in particular, that the intersecting faces have the same dimension.[1]

A "maximal simplex" (or facet) of K is a simplex that is not a face of another simplex in K. Note that due to the condition 1) above, it is sufficient to provide the list of all maximal simplices to fully determine the simplicial complex as taking the power set (the set of all subsets) of all maximal simplices generates the entire set of simplices in K. For the previous example $K = \langle [x_0x_1x_2] \rangle$, where $\langle \cdot \rangle$ denotes taking the power set. Without additional structure, providing the set of maximal faces is the most efficient way to communicate a simplicial complex.

Let f_p denote the number of p-simplices in K. It is convenient to collect all these by defining the f-vector of a simplicial complex:

$$f := (f_0, f_1, \ldots, f_{\dim(K)}), \tag{1.1.3}$$

where $\dim(K)$ is the dimension of K, defined to be the highest dimension of its simplices (note that $\dim(K) \leq n$ if there are $n+1$ vertices in K).

There are many methods to represent a simplicial complex, K. One way is simply to list every simplex in K.[2] However, this method of describing a simplicial complex is not efficient. In particular, if there are N_K simplices in K, then there exist descriptions of K that require only $\log(N_K)$ bits to describe. These include describing K by its maximal faces[3] or by its minimal non-faces.[4] The main focus of this work is simplicial complexes which are defined by a graph G (see subsection 1.1.2 for a definition), where the natural representation of K is simply the graph G.

We have described what is known as an *abstract* simplicial complex, defined combinatorially as a collection of sets without any reference to geometry or topology. However, given an abstract simplicial complex one can always associate a *geometric* simplicial complex by thinking of $[x_0x_1 \cdots x_p]$ as representing the convex hull of $(p+1)$ points in $\mathbb{R}^d$ with $d \geq \dim(K) + 1$. See [3] for more details and formal definitions. It thus makes sense to ask whether a simplicial complex has a k-dimensional hole. Intuitively, a hole in a space is a closed cycle which is non-contractible. Homology is what allows one to define this formally.

The boundary operator. The main insight in homology theory, and a precursor to many ideas in modern mathematics, is that one can attach an Abelian group structure to a simplicial complex. Given a simplicial

[1] We emphasize that two simplices must intersect at a *single* face of each simplex. For instance, two vertices connected by an edge, $\{[x_0], [x_1], [x_0x_1]\}$, is a simplicial complex but two points connected by two edges $\{[x_0], [x_1], [x_0x_1], [x_0x_1]\}$ is not because the two 1-simplices intersect at two faces. Two points connected by two edges is instead an example of a non-simplicial CW-complex (sometimes referred to as a 'bigon').

[2] As noted in the introduction, if K is input in this form then the homology problem is in P [1].

[3] The homology problem with K input as maximal faces is the version of the problem that was posed in [2].

[4] As a corollary of our main theorem we show that the homology problem with K input as minimal non-faces is QMA_1-hard.

complex K let K_p denote the set of all p-simplices, $K_p := \{\sigma_0^{(p)}, \sigma_1^{(p)}, \cdots, \sigma_{f_p}^{(p)}\}$. These are taken to be the generators of a collection of Abelian groups. The "p-chain groups" are then

$$C_p(K) := (K_p, +)\,, \tag{1.1.4}$$

where $+$ denotes the formal "addition" operation in the group. A general element of $C_p(K)$ is then given by

$$c^{(p)} = \alpha_0\, \sigma_0^{(p)} + \cdots + \alpha_{f_p}\, \sigma_{f_p}^{(p)}\,, \qquad \alpha_i \in \mathbb{F}\,, \tag{1.1.5}$$

where the coefficients α_i take value in a field $\mathbb{F}$ called the "coefficient field." The inverse element of $\sigma^{(p)}$, denoted formally by $-\sigma^{(p)}$, is obtained by reversing the orientation of $\sigma^{(p)}$ so that $\sigma^{(p)} + (-\sigma^{(p)}) = 0$.

One now introduces the "boundary operators" ∂_p, which formalizes the notion of boundary. Given a p-simplex $\sigma^{(p)} = [x_0 \cdots x_p]$, the action of the boundary operator is, by definition,

$$\partial_p [x_0 \cdots x_p] = \sum_{i=1}^{p} (-1)^i [x_0 \cdots \hat{x}_i \cdots x_p]\,, \tag{1.1.6}$$

where the notation $[x_0 \cdots \hat{x}_i \cdots x_p]$ means that the vertex x_i is deleted and the sum is to be understood in the sense above. That is, the boundary map acting on $\sigma^{(p)}$ gives a formal sum of all the boundary components of $\sigma^{(p)}$; the signs appearing on the RHS of (1.1.6) are such that the orientation of the boundary simplices are consistent with those of $\sigma^{(p)}$.[5] It is easy to see that

$$\partial_p \cdot \partial_{p+1} = 0\,, \tag{1.1.7}$$

reflecting the intuitive notion that the "boundary of a boundary" vanishes.

One can extend the action of ∂_p by linearity to a general p-chain (1.1.5). Thus, the operators ∂_p are a collection of homomorphisms between chain groups:

$$\partial_p : C_p(K) \to C_{p-1}(K)\,. \tag{1.1.8}$$

Given this (finite) collection of groups C_p and the boundary maps, it is convenient to introduce the notion of a "chain complex," which is a sequence of Abelian groups connected by the action of the boundary operator:[6]

$$C(K): \qquad 0 \to C_n(K) \xrightarrow{\partial_n} C_{n-1}(K) \xrightarrow{\partial_{n-1}} \cdots \xrightarrow{\partial_2} C_1(K) \xrightarrow{\partial_1} C_0(K) \xrightarrow{\partial_0} 0\,. \tag{1.1.9}$$

Note that since the $C_p(K)$ come equipped with a basis $\sigma^{(p)}$, the operators ∂_p can be expressed as matrices. In particular, one can define the "coboundary" operators

$$\partial_p^\dagger : C_{p-1} \to C_p \tag{1.1.10}$$

by hermitian conjugation of the matrix associated to ∂_p. These can be used to define a "co-chain" complex in which the direction of the arrows above is reversed.

Cycles, boundaries, and homology Two important notions are those of "cycles" and "boundaries." Consider the set of p-chains which are in the kernel of the boundary operator ∂_p. These are known as p-cycles and denoted by Z_p:

$$Z_p := \ker(\partial_p) = \{c^{(p)} \in C_p \mid \partial_p c^{(p)} = 0\}\,. \tag{1.1.11}$$

[5] For instance, for the solid triangle, $\partial[x_0x_1x_2] = [x_1x_2] - [x_0x_2] + [x_0x_1] = [x_0x_1] + [x_1x_2] + [x_2x_0]$, consistent with the orientations of each boundary edge–see Fig. 1.1.

[6] The trivial group at the left of C_n is included to emphasize the chain is finite.

Intuitively, these correspond to closed cycles in the simplicial complex, as they have no boundary. The space of p-cycles in fact forms a subgroup of C_p, as can be easily checked.

Consider now the set of p-chains which are in the image of the boundary operator ∂_{p+1}. These are known as p-boundaries and denoted by B_p:

$$B_p := \mathrm{im}(\partial_{p+1}) = \{c^{(p)} \mid c^{(p)} = \partial c^{(p+1)}\}\,. \tag{1.1.12}$$

Intuitively, these correspond to chains which are boundaries of a higher-dimensional chain. These also form a subgroup of C_p, as can be easily checked. In fact, B_p is a subgroup of Z_p,

$$B_p \subseteq Z_p\,, \tag{1.1.13}$$

which follows directly from (1.1.7). Again, this is simply the statement that boundaries do not themselves have a boundary.

With these elements one can now define the notion of homology. The p-th homology group is defined as the coset groups

$$H_p(K,\mathbb{F}) := \frac{Z_p}{B_p} = \frac{\ker(\partial_p)}{\mathrm{im}(\partial_{p+1})}\,. \tag{1.1.14}$$

That is, $H_p(K,\mathbb{F})$ denotes the set of all p-cycles which are not p-boundaries. This captures the intuitive notion of a p-dimensional hole in K. The number of independent p-dimensional holes is captured by the Betti numbers:

$$\beta_p = \mathrm{rank}\, H_p(K,\mathbb{F})\,. \tag{1.1.15}$$

The homology group takes the form $H_*(K,\mathbb{F}) = (\mathbb{F})^{\beta_0} \oplus (\mathbb{F})^{\beta_1} \oplus \cdots \oplus (\mathbb{F})^{\beta_n} \oplus T(K,\mathbb{F})$ where $T(K,\mathbb{F})$ are known as the torsion coefficients. The Betti numbers capture the freely acting part of the homology group while the torsion coefficients capture a possible non-freely acting part. These depend on the field coefficient $\mathbb{F}$ and the torsion vanishes for $\mathbb{F} = \mathbb{Q}, \mathbb{R}, \mathbb{C}$. Since we will always be working with $\mathbb{F} = \mathbb{C}$ we ignore torsion and the homology is completely specified by the Betti numbers: that is, $H_p(K,\mathbb{C}) = (\mathbb{C})^{\beta_p}$.

Recall that coset groups correspond to equivalence classes. The meaning of the coset above is that any two elements $c^{(p)}$ and $c^{(p)'}$ in Z_p which differ by a boundary are taken to be equivalent or "homologous":

$$c^{(p)} \sim c^{(p)'} \qquad \text{if} \qquad c^{(p)'} = c^{(p)} + \partial c^{(p+1)}\,. \tag{1.1.16}$$

The elements $c^{(p)}$ and $c^{(p)}$ are thus equivalent in homology and either one is a valid representative of the homology class.

Cycles which are boundaries are trivial elements of homology:

$$c^{(p)} = \partial c^{(p+1)} \sim 0\,. \tag{1.1.17}$$

The most important property of homology groups is that they are topological invariants of K; if two spaces K and M are homeomorphic, then $H_p(K,\mathbb{F}) = H_p(M,\mathbb{F})$. In fact, homology groups are not only homeomorphism invariants but homotopy invariants [4].

Note that determining whether a space has a non-trivial k-dimensional homology class[7] is then is then a question in linear algebra, studying the kernel and image of the linear operator ∂ [1]. This can be answered by bringing the boundary operator into a Smith normal form and thus homology is algorithmically computable but can be extremely slow for large matrices.

[7] Or, less formally, determining whether a space has a k-dimensional hole.

A useful quantity is the Euler characteristic of K, given by the alternating sum of Betti numbers:

$$\chi(K) = \sum_p (-1)^p \beta_p \,. \tag{1.1.18}$$

Since the Betti numbers are topological invariants, so is the Euler characteristic. The Euler-Poincaré formula states that it can can also be written as the alternating sum of the number of simplices at each dimension:

$$\chi(K) := \sum_p (-1)^p f_p \,. \tag{1.1.19}$$

Since no knowledge of the homology groups is required in this expression, this sometimes makes the Euler quantity an easier, albeit less refined, topological invariant to compute.

Reduced homology. It is sometimes useful to consider a slight modification called "reduced homology." This is defined by taking the augmented chain complex

$$0 \to C_n(K) \xrightarrow{\partial_n} C_{n-1}(K) \xrightarrow{\partial_{n-1}} \cdots \xrightarrow{\partial_2} C_1(K) \xrightarrow{\partial_1} C_0(K) \xrightarrow{\epsilon} \mathbb{F} \to 0 \,, \tag{1.1.20}$$

where $\epsilon(\sum \alpha_i \sigma_{0,i}) := \sum_i \alpha_i$. The corresponding homology groups $\tilde{H}_p(K, \mathbb{F})$ are defined analogously and one has

$$H_0(K, \mathbb{F}) = \tilde{H}_0(K, \mathbb{F}) \oplus \mathbb{F} \,, \qquad H_p(K, \mathbb{F}) = \tilde{H}_p(K, \mathbb{F}) \,, \qquad p \geq 1 \,. \tag{1.1.21}$$

The corresponding Euler characteristic $\tilde{\chi}$ is defined analogously. It is easy to see that it is related to the standard Euler characteristic by

$$\tilde{\chi}(K) = -\chi(K) + 1 \,. \tag{1.1.22}$$

As we discuss in Section 2.1 reduced homology groups capture the zero energy states of supersymmetric many-body systems and the reduced Euler characteristic corresponds to the so-called Witten index.

We will focus on homology with coefficients in $\mathbb{F} = \mathbb{C}$ (and thus $T(K, \mathbb{F}) = 0$) and to simplify notation we write

$$H_*(K) := H_*(K, \mathbb{C}) \,, \qquad \tilde{H}_*(K) := \tilde{H}_*(K, \mathbb{C}) \,. \tag{1.1.23}$$

1.1.2 The Clique/Independence Complex

Given a simple graph[8] $G = (V, E)$, the "clique complex" $Cl(G)$ is a simplicial complex whose k-simplices are given by $(k+1)$-cliques of G (i.e., complete subgraphs of G with $k+1$ vertices). Since any subgraph of a clique is a clique, the set $Cl(G)$ is closed under taking subsets and satisfies the first requirement of a simplicial complex. It is also easy to see it satisfies the second requirement. The vertices in the graph are given some ordering, which induces an orientation on the simplices. The action of the boundary operator is that in (1.1.6), sending k-cliques to $(k-1)$-cliques. Finding k-dimensional holes in clique complexes is an important task in TDA, with many applications including neuroscience [5–7] and the study of protein networks.

Another simplicial complex which is defined naturally given a graph G is the "independence complex" $I(G)$. The k-simplices of $I(G)$ are given by $(k+1)$-independent sets of G (i.e., a subset of $k+1$ disjoint vertices in G). Clearly, k-independent sets of G are equivalent to k-cliques of the complement graph $\bar{G}$ and therefore

$$I(G) = Cl(\bar{G}) \,. \tag{1.1.24}$$

[8] A simple graph is a graph that does not have more than one edge between any two vertices, and where no edge starts and ends on the same vertex.

Since the graph complement can be computed in time polynomial in $|V|$, the computational complexity of computing homology for the clique complex is equivalent to that of the independence complex. Throughout most of Section 1.3 we will focus on the independence complex, and in the final theorem we will translate our result to discuss the clique complex. It is worth noting that for $k > 2$ identifying k-cliques (independent sets) is NP-hard, so finding the clique (independence) complex of a graph G given the graph as input is in general NP-hard.

1.2 QMA_1 and Quantum k-SAT

In this section, we review the complexity class QMA_1 and quantum k-SAT, the archetypal QMA_1-complete problem [8]. As we discuss below, the definition of this class depends on the choice of a universal gate set $\mathcal{G}$ and we introduce a choice which will be used for our hardness proof in Section 1.3.

1.2.1 The complexity class QMA_1

The quantum complexity class QMA_1 is defined as the the perfect completeness version of QMA. Precisely,

Definition 1 (QMA_1 [8, 9])**.** *A promise problem $A = (A_{yes}, A_{no})$ is in QMA_1 if there exists a polynomial-time quantum circuit (the "verifier") V_x composed of gates from the gate set $\mathcal{G}$ for any n-bit input string x such that*

- *If $x \in A_{yes}$, there exists a $\mathsf{poly}(n)$-qubit witness state $|w\rangle$ such that $\Pr[V_x(|w\rangle) = 1] = 1$,*
- *If $x \in A_{no}$, then for any $\mathsf{poly}(n)$-qubit witness state $|w\rangle$, $\Pr[V_x(|w\rangle) = 1] \leq \frac{1}{3}$.*

There are two main differences with respect to the more standard class QMA. The first is that in the case of YES instances the verifier is required to accept an appropriate witness with probability 1, while in QMA this is only required to be some constant greater than 1/2 (and often taken to be 2/3). This is why this class is often referred to as perfect completeness or one-sided error version of its more common sibling QMA. Importantly, also note that the definition explicitly depends on the choice of a universal gate set $\mathcal{G}$. In the case of QMA the definition is independent of any choice of gate set, since all universal gate sets can approximate any unitary evolution. But for QMA_1 it is no longer necessarily enough to be able to approximate a given unitary. And for this reason when specifying the class QMA_1 it is necessary to define it relative to some particular choice of universal gate set.

A frequently used choice is $\mathcal{G}' = \{\mathrm{CNOT}, \hat{H}, T\}$ where

$$\mathrm{CNOT} = \begin{pmatrix} 1 & 0 & 0 & 0 \\ 0 & 1 & 0 & 0 \\ 0 & 0 & 0 & 1 \\ 0 & 0 & 1 & 0 \end{pmatrix}, \qquad \hat{H} = \frac{1}{\sqrt{2}} \begin{pmatrix} 1 & 1 \\ 1 & -1 \end{pmatrix}, \qquad T = \begin{pmatrix} 1 & 0 \\ 0 & e^{\frac{i\pi}{4}} \end{pmatrix} \tag{1.2.1}$$

However, for reasons to be discussed below we wish to have gates with *rational* coefficients. As shown in [10, Theorem 3.3] (it also follows from [11, Theorem 1.2]), the gate CNOT together with a one-qubit real unitary U is universal provided U^2 is basis-changing.

Our definition of QMA_1 is then based on the choice of universal gate set

$$\mathcal{G} = \{\mathrm{CNOT}, \mathrm{Toffoli}, U_{Pyth.}\} \qquad U_{Pyth.} = \frac{1}{5} \begin{pmatrix} 3 & 4 \\ -4 & 3 \end{pmatrix}, \tag{1.2.2}$$

for which all gates have rational coefficients. We note that choosing a gate set $\mathcal{G}' = \{\mathrm{Toffoli}, U_{Pyth.}\}$ would have led to the same complexity class since a CNOT gate can be exactly implemented using Toffoli gates. However, explicitly including the CNOT gate in our gate set simplifies the calculations for demonstrating clique density

(see subsection 1.3.3). We refer to $U_{Pyth.}$ as the "Pythagorean" gate, since any Pythagorean triple defines such a matrix. It is relative to this definition of QMA_1 that we will prove hardness of the clique homology problem.

The question of whether QMA_1 is strictly contained within QMA is open. The complexity classes are known to be distinct relative to a particular quantum oracle [12]. However, the versions of QMA and QMA_1 where the proofs are restricted to be classical bit strings *are* equal, for certain choices of universal gate sets in the perfect completeness case [13]. Equivalence of the classes for certain choices of universal gate set is also known to be true in the setting where there is exponentially small completeness-soundness gap [14]. Therefore, it has been argued that there is evidence both in favour of the two classes being equal, and against it.

1.2.2 Review of quantum k-SAT and the clock Hamiltonian

The archetypal QMA_1-complete problem is Quantum k-SAT:

Definition 1 (Quantum k-SAT [8])
Input: A set of k-local projectors $\Pi_S \in \mathcal{P}$ where S are possible subsets of $\{1, \ldots, n\}$ of cardinality k, and $\mathcal{P}$ are a set of projectors obeying certain constraints.
Promise: Either there exists a state $|\psi\rangle$ such that $\Pi_S |\psi\rangle = 0$ for all S or otherwise $\sum_S \langle\psi| \Pi_S |\psi\rangle \geq \epsilon$ for all $|\psi\rangle$, with $\epsilon > \frac{1}{\mathsf{poly}(n)}$.
Problem: Output YES if the former and NO if the latter.

It was shown in [8] that quantum k-SAT is QMA_1-complete for $k \geq 4$ and that for $k = 2$ there is an efficient classical algorithm to solve the problem. For $k = 3$ the problem was shown to be QMA_1-complete in [9]. We will construct a mapping from the construction of [8] to the k-local homology problem.

Comment on completeness. We have been deliberately vague about the definition of the set of allowable projectors $\mathcal{P}$ in the definition of quantum k-SAT. There is no need to put any constraints on the set of projectors $\mathcal{P}$ for showing that the problem is QMA_1-hard. However, for showing *containment* in QMA_1 care has to be taken, and the choice of $\mathcal{P}$ which ensures containment will depend on the universal gate set chosen in the definition of QMA_1. It is known that quantum k-SAT is contained in QMA_1 as long as there exists an efficient algorithm which can be used to measure the eigenvalue of any $\Pi \in \mathcal{P}$ for arbitrary state $|\psi\rangle$ using the gate set $\mathcal{G}$ [8, 9]. And clearly to show QMA_1 completeness it is necessary to demonstrate that the set of projectors used in mapping from a QMA_1 verification circuit to quantum k-SAT is contained in $\mathcal{P}$. Since throughout this work we are concerned with demonstrating QMA_1-hardness, not containment or completeness, we will defer any further discussion of the choice of $\mathcal{P}$ and allow it to contain arbitrary k-local projectors.

1.2.3 Mapping from quantum 4-SAT to a local Hamiltonian

The construction in [8] maps a quantum circuit, $U = U_L \cdots U_2 U_1$, $U_j \in \mathcal{G}$ operating on N qubits into the ground state of a local Hamiltonian $H(U)$ acting on Hilbert space $\mathcal{H}_{\text{clock}} \otimes \mathcal{H}_{\text{comp}}$ where $\mathcal{H}_{\text{clock}} = (\mathbb{C}^4)^{\otimes L}$ and $\mathcal{H}_{\text{comp}} = (\mathbb{C}^2)^{\otimes N}$. The ground state of $H(U)$ is a 'history state' [45] of the form:

$$|\Omega(\psi_{wit})\rangle = \frac{1}{T} \sum_{t=1}^{L} |t\rangle |\psi_t\rangle \tag{1.2.3}$$

where $|\psi_t\rangle = \Pi_{i=1}^{t} U_i |\psi_{wit}\rangle$ and $|t\rangle$ is an orthonormal basis for $\mathcal{H}_{\text{clock}}$.

A single clock particle in [8] has four possible basis states - $|u\rangle = |00\rangle$ - unborn, $|a_1\rangle = |01\rangle$ - active phase one, $|a_2\rangle = |10\rangle$ - active phase two and $|d\rangle = |11\rangle$ - dead. As time 'passes' each clock particle evolves from the unborn state, through the two active stages, and eventually to the dead state. 'Legal' clock states are defined as those obeying certain constraints [8]:

1. The first clock particle is either active or dead
2. The last clock particle is either unborn or active.
3. There is at most one active clock particle
4. If clock particle j is dead then all particles k satisfying $1 \leq k \leq j$ are also dead

In [8] it is shown that the ground space of the Hamiltonian $H_{\text{clock}} = \sum_{j=1}^{6} H_{\text{clock}}^{(j)}$ is spanned by legal clock states, where:

$$H_{\text{clock}}^{(1)} = |u\rangle \langle u|_1 \tag{1.2.4}$$

$$H_{\text{clock}}^{(2)} = |d\rangle \langle d|_L \tag{1.2.5}$$

$$H_{\text{clock}}^{3} = \sum_{1 \leq j \leq k \leq L} \left(|a_1\rangle \langle a_1| + |a_2\rangle \langle a_2|\right)_j \otimes \left(|a_1\rangle \langle a_1| + |a_2\rangle \langle a_2|\right)_k \tag{1.2.6}$$

$$H_{\text{clock}}^{(4)} = \sum_{1 \leq j \leq k \leq L} \left(|a_1\rangle \langle a_1| + |a_2\rangle \langle a_2| + |u\rangle \langle u|\right)_j \otimes \left(|d\rangle \langle d|\right)_k \tag{1.2.7}$$

$$H_{\text{clock}}^{(5)} = \sum_{1 \leq j \leq k \leq L} \left(|u\rangle \langle u|\right)_j \otimes \left(|a_1\rangle \langle a_1| + |a_2\rangle \langle a_2| + |d\rangle \langle d|\right)_k \tag{1.2.8}$$

$$H_{\text{clock}}^{(6)} = \sum_{1 \leq j \leq L-1} |d\rangle \langle d|_j \otimes |u\rangle \langle u|_{j+1} \tag{1.2.9}$$

The computational qubits can be divided into input data and witness registers, R_{in} and R_{wit} such that $|R_{in}| + |R_{wit}| = N$. The input qubits are initialised into the all zero state at time zero via:

$$H_{\text{in}} = |a_1\rangle \langle a_1|_1 \otimes \left(\sum_{b \in R_{in}} |1\rangle \langle 1|_b \right) \tag{1.2.10}$$

The 'propagation' Hamiltonian is defined as:

$$H_{\text{prop}} = \sum_{t=1}^{L} \left(H_{\text{prop,t}} + H'_{\text{prop,t}} \right) \tag{1.2.11}$$

where:

$$H_{\text{prop,t}} = \frac{1}{2} \left[\left(|a_1\rangle \langle a_1| + |a_2\rangle \langle a_2|\right) \otimes \mathbb{I} - |a_2\rangle \langle a_1| \otimes U_t - |a_1\rangle \langle a_2| \otimes U_t^{\dagger} \right] \tag{1.2.12}$$

$$H'_{\text{prop,t}} = \frac{1}{2} \left(|a_2, u\rangle \langle a_2, u| + |d, a_1\rangle \langle d, a_1| - |d, a_1\rangle \langle a_2, u| - |a_2, u\rangle \langle d, a_1| \right) \tag{1.2.13}$$

It can easily be checked that the zero energy ground space of:

$$H(U) = H_{\text{in}} + H_{\text{clock}} + H_{\text{prop}} \tag{1.2.14}$$

is spanned by computational history states of the form:

$$|\Omega(\psi_{wit})\rangle = \sum_{t=1}^{L} \left(|d\rangle^{\otimes t-1} |a_1\rangle_t |u\rangle^{\otimes L-t} \otimes |Q_{t-1}\rangle + |d\rangle^{\otimes t-1} |a_2\rangle_t |u\rangle^{\otimes L-t} \otimes |Q_t\rangle \right) \tag{1.2.15}$$

where $|Q_0\rangle = |0\rangle^{\otimes R_{in}} \otimes |\psi_{wit}\rangle$, and $|Q_t\rangle = U_t |Q_{t-1}\rangle$, $t \in [1, L]$. Therefore the ground states of $H(U)$ encode the computational history of the circuit $U = U_L ... U_1$.

The final step is to penalise computational histories where the circuit rejects the witness, this is achieved using the projector:

$$H_{\text{out}} = |a_2\rangle \langle a_2|_L \otimes \left(\sum_{b \in R_{out}} |1\rangle \langle 1|_b \right) \tag{1.2.16}$$

This gives energy to computational history states $|\Omega(\psi_{wit})\rangle$ if the circuit U rejects the witness $|\psi_{wit}\rangle$ with non-zero probability.

So the final Hamiltonian:

$$H_{\text{Bravyi}} = H_{\text{in}} + H_{\text{clock}} + H_{\text{prop}} + H_{\text{out}} \tag{1.2.17}$$

has a zero energy ground state iff there exists a witness $|\psi_{wit}\rangle$ such that circuit U accepts with probability one.

1.2.4 Projectors needed to implement H_{Bravyi}

Here we outline the projectors needed to implement the clock construction of [8] using our universal gate set $\mathcal{G}$.

For each H_{in} only a single projector is needed.

$$H_{\text{in}} = |011\rangle \langle 011| \tag{1.2.18}$$

This is a three qubit projector of rank 1. H_{out} is equivalent, up to permuting the qubits involved in the interaction:

$$H_{\text{out}} = |101\rangle \langle 101| \tag{1.2.19}$$

Implementing H_{clock} requires six projectors. $H^{(1)}_{\text{clock}}$ and $H^{(2)}_{\text{clock}}$ are a two qubit projectors with rank 1:

$$H^{(1)}_{\text{clock}} = |00\rangle \langle 00| \tag{1.2.20}$$

$$H^{(2)}_{\text{clock}} = |11\rangle \langle 11| \tag{1.2.21}$$

The remaining terms in H_{clock} each act on 4 qubits. $H^{(3)}_{\text{clock}}$ and $H^{(5)}_{\text{clock}}$ each have rank 4, $H^{(4)}_{\text{clock}}$ has rank 3, and $H^{(6)}_{\text{clock}}$ has rank 1:

$$H^{(3)}_{\text{clock}} = |0101\rangle \langle 0101| + |0110\rangle \langle 0110| + |1001\rangle \langle 1001| + |1010\rangle \langle 1010| \tag{1.2.22}$$

$$H^{(4)}_{\text{clock}} = |0111\rangle \langle 0111| + |1011\rangle \langle 1011| + |0011\rangle \langle 0011| \tag{1.2.23}$$

$$H^{(5)}_{\text{clock}} = |0001\rangle \langle 0001| + |0010\rangle \langle 0010| + |0011\rangle \langle 0011| \tag{1.2.24}$$

$$H^{(6)}_{\text{clock}} = |1100\rangle \langle 1100| \tag{1.2.25}$$

For H_{prop} we have to consider two projectors for $H_{\text{prop,t}}$ and one for $H'_{\text{prop,t}}$. The projector for propagation under the pythagorean gate is a three qubit projector of rank 2 given by:

$$
\begin{aligned}
H_{\mathrm{prop,t}}(U_{Pyth.}) = \frac{1}{2}[(|01\rangle\langle 01| + |10\rangle\langle 10|) \otimes \mathbb{I} \\
-\frac{1}{5}(3\,|100\rangle\langle 010| - 4\,|100\rangle\langle 011| + 4\,|101\rangle\langle 010| + 3\,|101\rangle\langle 011|) \\
-\frac{1}{5}(3\,|010\rangle\langle 100| + 4\,|010\rangle\langle 101| - 4\,|011\rangle\langle 100| + 3\,|011\rangle\langle 101|)]
\end{aligned} \tag{1.2.26}
$$

The projector for evolution under CNOT is a four qubit projector of rank 4:

$$
\begin{aligned}
H_{\mathrm{prop,t}}(CNOT) = \frac{1}{2}[(|01\rangle\langle 01| + |10\rangle\langle 10|) \otimes \mathbb{I} \\
-(|1000\rangle\langle 0100| + |1001\rangle\langle 0101| + |1010\rangle\langle 0111| + |1011\rangle\langle 0110|) \\
-(|0100\rangle\langle 1000| + |0101\rangle\langle 1001| + |0110\rangle\langle 1011| + |0111\rangle\langle 1010|)]
\end{aligned} \tag{1.2.27}
$$

While the projection for evolution under the Toffoli gate is a five qubit projector of rank 8:

$$
\begin{aligned}
H_{\mathrm{prop,t}}(\mathrm{Toffoli}) = \frac{1}{2}[(|01\rangle\langle 01| + |10\rangle\langle 10|) \otimes \mathbb{I} \\
-(|10000\rangle\langle 01000| + |10001\rangle\langle 01001| + |10010\rangle\langle 01010| + |10011\rangle\langle 01011| \\
+|10100\rangle\langle 01100| + |10101\rangle\langle 01101| + |10110\rangle\langle 01111| + |10111\rangle\langle 01110|) \\
-(|01000\rangle\langle 10000| + |01001\rangle\langle 10001| + |01010\rangle\langle 10010| + |01011\rangle\langle 10011| \\
+|01100\rangle\langle 10100| + |01101\rangle\langle 10101| + |01110\rangle\langle 10111| + |01111\rangle\langle 10110|)
\end{aligned} \tag{1.2.28}
$$

And finally $H'_{\mathrm{prop,t}}$ is a four qubit projector with rank 1:

$$
H'_{\mathrm{prop,t}} = \frac{1}{2}(|1000\rangle\langle 1000| + |1101\rangle\langle 1101| - |1101\rangle\langle 1000| - |1000\rangle\langle 1101|) \tag{1.2.29}
$$

In our reduction from QUANTUM k-SAT to homology we implement each of the projectors that make up H_{Bravyi} by decomposing it into rank one projectors, and implementing these. We have summarized the rank-1 projectors which are required in order to construct H_{Bravyi} for the universal gate set (1.2.2) in Table 1.1.

1.3 Clique Homology is QMA_1-hard

In this Section, we prove our main result Theorem **??**. For purposes of presentation we will focus on the independence complex $I(G)$, rather than the clique complex. As noted in subsection 1.1.2 these are related by taking the graph complement, which can be done efficiently in the size of the graph, and thus proving QMA_1-hardness for the independence complex or the clique complex is equivalent. In subsection 1.3.2 we will explicitly consider the mapping between the two problems.

As outlined in the Introduction, the basic idea is to encode the computational history of a QMA_1 verification circuit into the topology of an independence complex. We achieve this via the "circuit-to-Hamiltonian" construction reviewed in Section 1.2. In Table 1.1 we have outlined all the rank-one projectors that can appear in the Hamiltonian we want to implement, i.e. every Hamiltonian we want to implement can be written as a sum of terms from Table 1.1 The task at hand is then to construct modular graphs (which we refer to as gadgets) which implement each of the rank-one projectors in Table 1.1 in the sense that the independence complex of the graph is isomorphic to the ground state of the corresponding projector. Once we have constructed these gadgets we then show how to implement sums and tensor products of projectors. This allows us to construct a graph G such

Term in H_{Bravyi}	*Penalizes state* $\ket{\psi_S}$
$H'_{\text{prop,t}}$	$\frac{1}{\sqrt{2}}\ket{10}(\ket{11}-\ket{00})$
$H_{\text{prop,t}}(\text{CNOT})$	$\frac{1}{\sqrt{2}}\ket{01}(\ket{10}-\ket{01})$
$H_{\text{prop,t}}(\text{CNOT})$	$\frac{1}{\sqrt{2}}\ket{00}(\ket{10}-\ket{01})$
$H_{\text{prop,t}}(\text{Toffoli})$	$\frac{1}{\sqrt{2}}\ket{000}(\ket{10}-\ket{01})$
$H_{\text{prop,t}}(\text{Toffoli})$	$\frac{1}{\sqrt{2}}\ket{101}(\ket{10}-\ket{01})$
$H_{\text{prop,t}}(\text{Toffoli})$	$\frac{1}{\sqrt{2}}\ket{010}(\ket{10}-\ket{01})$
$H_{\text{prop,t}}(U_{Pyth.})$	$\frac{1}{5\sqrt{2}}(-5\ket{011}+4\ket{100}+3\ket{101})$
$H_{\text{prop,t}}(U_{Pyth.})$	$\frac{1}{5\sqrt{2}}(-5\ket{010}+3\ket{100}-4\ket{101})$
$H_{\text{prop,t}}(\text{CNOT})$	$\frac{1}{\sqrt{2}}\ket{1}(\ket{101}-\ket{010})$
$H_{\text{prop,t}}(\text{Toffoli})$	$\frac{1}{\sqrt{2}}\ket{11}(\ket{101}-\ket{010})$
$H_{\text{prop,t}}(\text{CNOT})$	$\frac{1}{\sqrt{2}}\ket{1}(\ket{011}-\ket{100})$
$H_{\text{prop,t}}(\text{Toffoli})$	$\frac{1}{\sqrt{2}}\ket{11}(\ket{011}-\ket{100})$
$H^{(1)}_{\text{clock}}$	$\ket{00}$
$H^{(2)}_{\text{clock}}$	$\ket{11}$
H_{in}, H_{out}	$\ket{011}$
$H^{(6)}_{\text{clock}}$, $H^{(4)}_{\text{clock}}$, $H^{(5)}_{\text{clock}}$, $H^{(3)}_{\text{clock}}$	$\ket{1100}$
$H^{(4)}_{\text{clock}}$	$\ket{0111}$
$H^{(5)}_{\text{clock}}$	$\ket{0001}$

Table 1.1: The rank-1 projectors which are required in order to construct H_{Bravyi} from [8] with universal gate set $\mathcal{G}$. The set includes 5-local projectors because $\mathcal{G}$ includes a 3-local gate (whereas the universal gate set in [8] only includes 1- and 2-local gates). Note we collated projectors which are the same up to re-ordering the qubits involved, i.e. we treat the projectors onto $\ket{01}$ and $\ket{10}$ as equivalent.

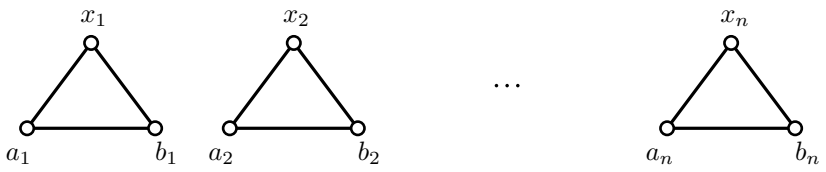

Figure 1.2: A graph G_n representing a system of n disconnected triangles. We will order the vertices (and hence induce an orientation on the simplices in the indepdendence complex) by $x_i > a_i > b_i$ and $\alpha_i > \beta_j$ for $i < j$ and for $\alpha, \beta \in \{x, a, b\}$.

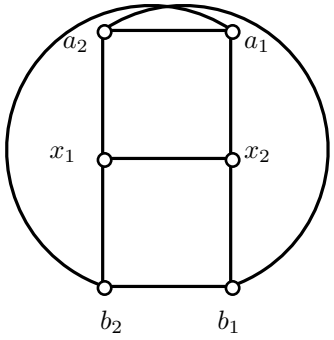

Figure 1.3: The independence complex $I(G_2)$ associated to two disjoint triangles.

that the corresponding independence complex has a nontrivial homology if and only if the Hamiltonian H_{Bravyi} has a zero energy groundstate.[9]

1.3.1 Basic gadgets

Consider a graph G_n consisting of n disconnected triangles (see Fig. 1.2) and denote the associated independence complex by $\Sigma_n := I(G_n)$. The total number of independent sets is 4^n. The largest independent sets are of size n and there are 3^n of them, corresponding to choosing one vertex from each triangle. We claim that the homology groups for all $n \geq 2$ are given by

$$H_0(\Sigma_n) \cong \mathbb{C}\,, \qquad H_{n-1}(\Sigma_n) \cong (\mathbb{C}^2)^{\otimes n}\,, \qquad H_{i\neq\{0,n-1\}}(\Sigma_n) \cong 0\,. \tag{1.3.1}$$

Thus, the $(n-1)^{\text{th}}$ homology group of Σ_n is isomorphic to the Hilbert space of n qubits. It is inside this vector space that we will encode the satisfying instances of quantum k-SAT.

Consider as a simple example the case of two triangles, $n = 2$. There are a total of 6 independent sets of size 1 and 9 independent set of size 2, corresponding to the vertices and edges of Σ_2, respectively (see Fig. 1.3). Clearly, Σ_2 has one connected component, and thus $\beta_0 = 1$, and four independent 1-dimensional holes (1-dimensional non-contractible cycles), and thus $\beta_1 = 4$, while all other Betti numbers vanish, consistent with (1.3.1). The general result for arbitrary n is easy to show.[10]

[9] In fact, we will require the reduction to be parsimonious so there is a 1-to-1 correspondence between the number of accepting witnesses to the QMA_1 protocol and the rank of the homology group. This will allow us to show the counting version of the problem is #BQP-hard.

[10] One way to see this is by using the formula for reduced homology $\tilde{H}_k(K \cup L) = \sum_{p+q+1=k} H_p(K) \otimes H_q(L)$. It is straightforward to see that $\tilde{H}_0(\Sigma_1) = (\mathbb{C})^2$ and $\tilde{H}_i(\Sigma_1) = 0$ for all $i \geq 1$. The result above then follows from $\Sigma_n = \Sigma_1 \cup \cdots \cup \Sigma_1$ and using this expression recursively.

To make contact with standard qubit notation, we label the basis for $H_{n-1}(\Sigma_n)$ by the set of all n-bit strings. We note that such a canonical basis is obtained as follows. Let

$$|0\rangle_i := [x_i] - [a_i]\,, \qquad |1\rangle_i := [x_i] - [b_i]\,, \qquad i \in \{1 \cdots n\}\,. \tag{1.3.2}$$

where x_i, a_i, b_i label the vertices of each triangle (see Fig. 1.3). Note that each of these 0-chains is annihilated by the boundary operator,

$$\partial\,|0\rangle_i = 0\,, \qquad \partial\,|1\rangle_i = 0\,, \qquad i \in \{1 \cdots n\}\,. \tag{1.3.3}$$

Let us introduce some notation. Consider two simplices $\sigma^{(p)} = [x_0 \cdots x_p]$ and $\sigma^{(q)} = [y_0 \cdots y_q]$. We define the wedge product $\wedge$ as

$$\sigma^{(p)} \wedge \sigma^{(q)} = \begin{cases} [x_0 \cdots x_p y_0 \cdots y_q] & x_i \neq y_j \\ 0 & \text{otherwise} \end{cases} \tag{1.3.4}$$

Then, a basis $B = \{|e_i\rangle\,, i = 1 \cdots 2^n\}$ for $H_{n-1}(\Sigma_n)$ is obtained by

$$\begin{aligned} |0 \cdots 0\rangle &:= ([x_1] - [a_1]) \wedge \cdots \wedge ([x_n] - [a_n])\,, \\ |0 \cdots 1\rangle &:= ([x_1] - [a_1]) \wedge \cdots \wedge ([x_n] - [b_n])\,, \\ &\vdots \\ |1 \cdots 1\rangle &:= ([x_1] - [b_1]) \wedge \cdots \wedge ([x_n] - [b_n])\,. \end{aligned} \tag{1.3.5}$$

Indeed, each of the basis states $|e_i\rangle$ is an $(n-1)$-dimensional hole in Σ_n since each $\partial\,|e_i\rangle = 0$ and $|e_i\rangle \neq \partial\,|f_i\rangle$ since there are no $(n+1)$-independent sets $|f_i\rangle$ in G_n. Expanding the products, and $[ij] = -[ji]$ and $[ij] = [i] \wedge [j]$ one obtains the 2^n linear combinations spanning $H_{n-1}(\Sigma_n) \cong (\mathbb{C}^2)^{\otimes n}$.

1.3.1.1 2-qubit projectors

To illustrate this, consider the case $n = 2$. The corresponding simplicial complex Σ_2 consists of 6 vertices corresponding to the 6 1-independent sets and nine 1-simplices corresponding to the 9 2-independent sets of G_2 (see Fig. 1.4). Expanding the terms in (1.3.5), the computational basis for $H_1(\Sigma_2) = \mathbb{C}^4$ is

$$\begin{aligned} |00\rangle &= [x_1\, x_2] + [x_2\, a_1] + [a_1\, a_2] + [a_2\, x_1]\,, \\ |01\rangle &= [x_1\, x_2] + [x_2\, a_1] + [a_1\, b_2] + [b_2\, x_1]\,, \\ |10\rangle &= [x_1\, x_2] + [x_2\, b_1] + [b_1\, a_2] + [a_2\, x_1]\,, \\ |11\rangle &= [x_1\, x_2] + [x_2\, b_1] + [b_1\, b_2] + [b_2\, x_1]\,. \end{aligned} \tag{1.3.6}$$

These correspond to the four independent non-contractible 1-cycles in Σ_2 depicted in Fig. 1.4.

We now follow the general strategy outlined above. We begin with a simple example. Consider the rank-1 classical projector

$$\Pi = |00\rangle\langle 00|\,. \tag{1.3.7}$$

To eliminate the 1-dimensional hole corresponding to the state $|00\rangle$, we identify the cycle corresponding to this state in Σ_2, shown in the first diagram in Fig. 1.4. In order to fill this face we add a new "mediator" vertex m and the four 2-simplices $[a_1 a_2 m]$, $[a_2 x_1 m]$, $[x_1 x_2 m]$, and $[x_2 a_1 m]$. This results in filling in the 1-chain $|00\rangle$, which is thus no longer a hole in Σ_2' (see Fig. 1.5). Indeed, we can verify this algebraically:

$$|00\rangle = \partial\,|\Psi\rangle\,, \tag{1.3.8}$$

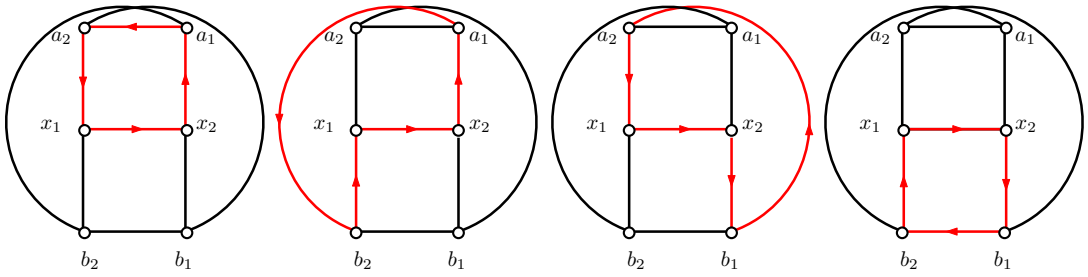

Figure 1.4: The independence complex $\Sigma_2 = I(G_2)$ associated to $n = 2$ non-interacting qubits. The simplicial complex has 4 independent 1-cycles, corresponding go $H_1(\Sigma_2) \cong \mathbb{C}^4$. The four basis states $\{|00\rangle, |01\rangle, |10\rangle, |11\rangle\}$ are indicated in red.

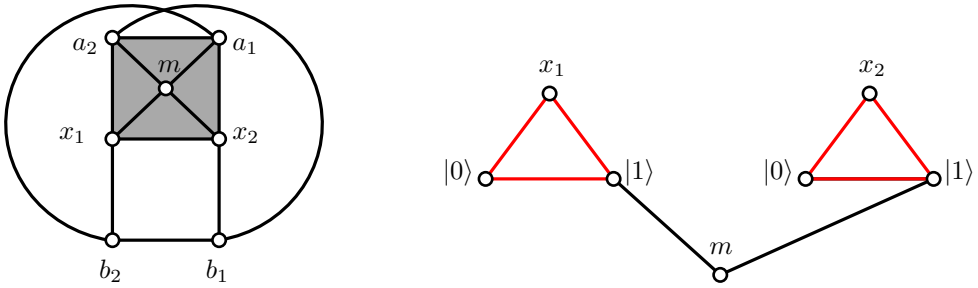

Figure 1.5: Filling in the face $|\Psi\rangle$ bounded by the cycle $|00\rangle$ leads to the simplex Σ_2', rendering the state $|00\rangle$ a trivial element of homology. This is accomplished by adding the additional vertex m and the 2-simplices $[a_1a_2m]$, $[a_2x_1m]$, $[x_1x_2m]$, and $[x_2a_1m]$. In the corresponding graph G_2' shown on the right this amounts to adding a mediator vertex and connecting it as depicted.

with

$$|\Psi\rangle = [a_1a_2m] + [a_2x_1m] + [x_1x_2m] + [x_2a_1m] \tag{1.3.9}$$

where $\partial = \partial_{a,b,x} + \partial_m$ is the boundary operator on Σ_2'. Finally, from Σ_2' we construct the graph G_2' such that $\Sigma_2' = I(G_2')$. It is easy to see that this corresponds to adding the mediator vertex m and connecting it to the vertices b_1 and b_2.

Projectors of higher rank are easily obtained. Consider for instance the rank-2 classical projector

$$\Pi = |00\rangle\langle 00| + |11\rangle\langle 11| \ . \tag{1.3.10}$$

Since this lifts both states $|00\rangle$ and $|11\rangle$ we need to fill the faces of the first and last cycle in Fig. 1.4, which is achieved by adding two mediator vertices m_1 and m_2 and eight 2-simplices. Explicitly,

$$|00\rangle = \partial\,|\Psi_1\rangle \ , \qquad |11\rangle = \partial\,|\Psi_2\rangle \tag{1.3.11}$$

with

$$\begin{aligned} |\psi_1\rangle &= [a_1a_2m_1] + [a_2x_1m_1] + [x_1x_2m_1] + [x_2a_1m_1]\,, \\ |\psi_2\rangle &= [x_1b_2m_2] + [b_2x_1m_2] + [x_1x_2m_2] + [x_1b_1m_2]\,. \end{aligned} \tag{1.3.12}$$

The resulting graph Σ_2' is shown in Table 1.2. Note that the total gadget is given by overlapping the corresponding graph gadgets on the common qubits and connecting the mediators. In subsection 1.3.1.8 we outline a general procedure for adding projectors which act on the same qubits.

Projectors which are not diagonal in the computational basis require a little more work. Consider the projector

$$\Pi = (|00\rangle - |11\rangle)(\langle 00| - \langle 11|)\,. \tag{1.3.13}$$

Note this is a rank-1 projector, lifting only the entangled state $|00\rangle - |11\rangle$, given by

$$|00\rangle - |11\rangle = [x_2\, a_1] + [a_1\, a_2] + [a_2\, x_1] + [x_1\, b_2] + [b_2\, b_1] + [b_1\, x_2]\,, \tag{1.3.14}$$

To fill in this (and *only* this) cycle by a triangulation of the enclosed face one requires three mediators, which is shown in Table 1.2. The corresponding graph G_2' is also shown there.[11] Again, one can algebraically check that

$$|00\rangle - |11\rangle = \partial\,|\Psi\rangle\ , \tag{1.3.15}$$

where

$$\begin{aligned}|\Psi\rangle = &([x_2\, a_1] + [a_1\, a_2]) \wedge [m_3] + ([a_2\, x_1] + [x_1\, b_2]) \wedge [m_1] + ([b_2\, b_1] + [b_1\, x_2]) \wedge [m_2] \\ &+ [b_2 m_2 m_1] + [x_2 m_3 m_2] + [a_2 m_1 m_3] + [m_1 m_2 m_3]\,.\end{aligned} \tag{1.3.16}$$

Furthermore, one can check that this is the *only* 1-cycle rendered trivial by this triangulation, as desired (see subsection 1.3.1.7). The projector $\Pi = (|01\rangle - |10\rangle)(\langle 01| - \langle 10|)$ is generated in the same way, up to relabelling (see Table 1.2).

1.3.1.2 3-qubit projectors

We now consider $n = 3$ and thus need to identify 2-dimensional voids in Σ_3 to be filled in. The easiest ones to identify are the classical projectors and we begin again with a simple example to illustrate the method. Consider the classical 3-qubit, rank-1, projector

$$\Pi = |000\rangle\langle 000|\ . \tag{1.3.17}$$

This classical basis state is a 2-cycle, given by:

$$|000\rangle = [x_1x_2x_3] + [x_1a_3x_2] + [a_2x_1x_3] + [x_1a_2a_3] + [a_1x_3x_2] + [a_1x_2a_3] + [a_1a_2x_3] + [a_2a_1a_3]\,. \tag{1.3.18}$$

The 2-cycle can be visualised as a double pyramid with vertices $\{x_{1,2,3}, a_{1,2,3}\}$ and whose 2-faces are given by the eight terms above.

To fill in this 2-cycle we add a single mediator vertex m and connect it to all 6 vertices. The eight triangles bounding the double pyramid, therefore now form tetrahedrons, meeting at the mediator vertex:

$$[x_1x_2x_3m], [x_1a_3x_2m], [a_2x_1x_3m], [x_1a_2a_3m], [a_1x_3x_2m], [a_1x_2a_3m], [a_1a_2x_3m], [a_2a_1a_3m] \tag{1.3.19}$$

The corresponding graph G_3' is simply three triangles all connected to the single mediator, shown in Table 1.3). One can easily algebraically check that

$$|000\rangle = \partial'\,|\Psi\rangle \tag{1.3.20}$$

where $|\Psi\rangle = |000\rangle \wedge [m]$ is the the equal superposition of the eight 4-simplices given in eq. (1.3.19) and $\partial' = \partial_{x,a,b} + \partial_m$. Thus rendering $|000\rangle$ a trivial element of homology.

[11] Note that there is a choice on how to perform this triangulation and the choice we have made breaks the symmetry between the two qubits.

2-qubit Projector	Gadget Σ_2'	Gadget G_2'
$\|00\rangle\langle 00\|$	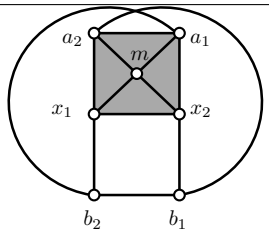	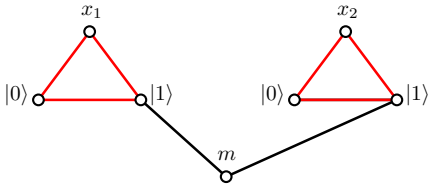
$\|00\rangle\langle 00\| + \|11\rangle\langle 11\|$	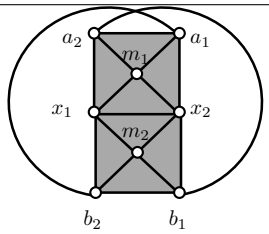	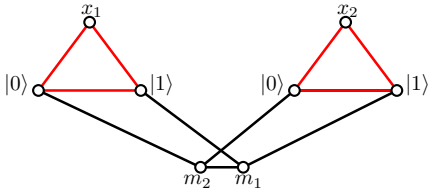
$(\|00\rangle - \|11\rangle)(\langle 00\| - \langle 11\|)$	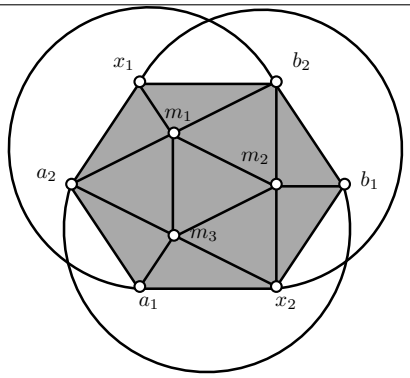	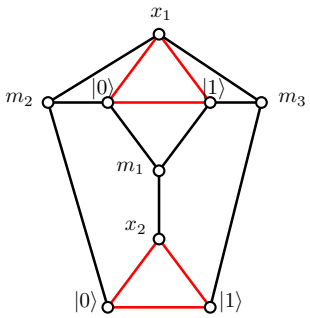
$(\|01\rangle - \|10\rangle)(\langle 01\| - \langle 10\|)$	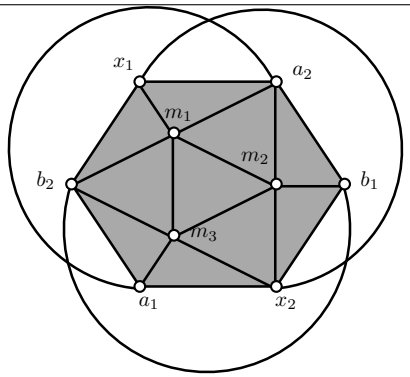	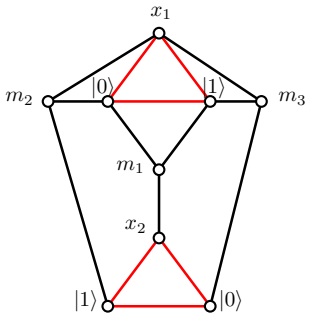

Table 1.2: Collection of gadgets for each 2-qubit projector in the clock Hamiltonian of quantum 4-SAT. The red triangles denote the qubits.

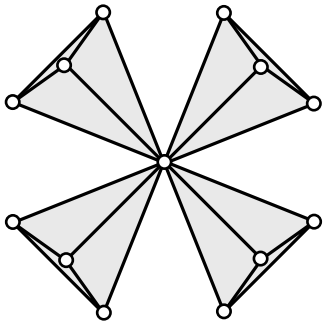

Figure 1.6: Four solid tetrahedra connected at a single mediator vertex m. The base of each tetrahedron is glued to a face in the 2-cycle to be filled in.

Crucially, one can check that no other 3-qubit state can be written in this form and thus the only lifted state is $|000\rangle$ (see subsection 1.3.1.7). The corresponding graph gadget G_3' is what one would expect and could have been guessed directly. However, directly guessing is no longer possible when looking for gadgets to uplift entangled states, which in general will contain an unwieldy number of mediator and connections.

1.3.1.3 The 3-qubit CNOT and Toffoli gadget

We now consider the projector

$$\Pi = (|101\rangle - |010\rangle)(\langle 101| - \langle 010|)\,, \tag{1.3.21}$$

which arises from the CNOT and Toffoli gates (see Table 1.1), lifting the entangled state $|101\rangle - |010\rangle$. This cycle can be thought of as adding $|101\rangle$ and $|010\rangle$ with opposite orientations (see Fig. 1.7). To fill in this cycle consider four solid tetrahedra connected at a common vertex m, as shown in Fig. 1.6. The base of each tetrahedron can be glued to to one of the faces in Σ_3. There are a total of 14 faces so we introduce 3 mediators $m_{1,2,3}$ and glue these to 12 different faces. This leaves two faces unfilled, which we fill by simply introducing two additional mediators m_4 and m_5 forming two tetrahedra with those two faces. This partially fills in the three-dimensional void, leaving some empty wedges between the 14 tetrahedra. To fill these spaces we simply connect all the mediators $m_1, \cdots, m_5$ by edges and fill the wedges in between by tetrahedra. The resulting simplicial complex consists of 14 0-simplices, 61 1-simplices, 97 2-simplices, 43 3-simplices, and 1 4-simplex (given by $[m_1...m_5]$). In this way the three-dimensional void has been completely filled in. As a simple consistency check we see that the Euler characteristic is $\chi = 1 - 14 + 61 - 97 + 43 - 1 = -7$, consistent with $H_2 = (\mathbb{C})^7$. The corresponding graph is shown in Table 1.3.

We can check algebraically that this procedure correctly fills in the desired void. The cycle to fill in is given by:

$$\begin{aligned} |101\rangle - |010\rangle = {} & [a_1 b_2 a_3] + [a_1 a_3 x_2] + [a_1 x_3 b_2] + [a_1 x_2 x_3] + [a_2 b_1 b_3] + [b_1 a_2 x_3] + [a_2 b_3 x_1] \\ & + [a_2 x_1 x_3] + [a_3 b_2 x_1] + [a_3 x_1 x_2] + [b_1 x_2 b_3] + [b_1 x_3 x_2] + [x_1 b_2 x_3] + [x_1 b_3 x_2] \end{aligned} \tag{1.3.22}$$

The first 3 mediators $m_{1,2,3}$ are glued to 12 of the faces from , as follows:

$$\begin{aligned} & ([b_1 a_2 x_3] + [b_1 x_2 x_3] + [a_1 b_2 x_3] + [a_1 x_2 x_3]) \wedge [m_1] \\ & ([x_1 a_2 b_3] + [x_1 a_2 x_3] + [x_1 b_2 x_3] + [x_1 b_2 a_3]) \wedge [m_2] \\ & ([x_1 x_2 b_3] + [b_1 x_2 b_3] + [x_1 x_2 a_3] + [a_1 x_2 a_3]) \wedge [m_3]\,. \end{aligned} \tag{1.3.23}$$

3-qubit Projector	Gadget Σ_3'	Gadget G_3'
$\|000\rangle\langle 000\|$	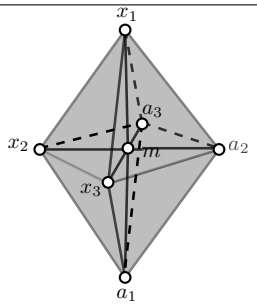	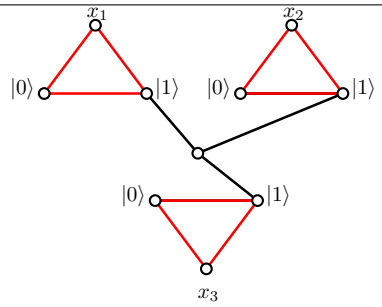
$\|001\rangle\langle 001\|$	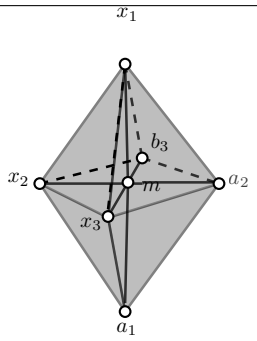	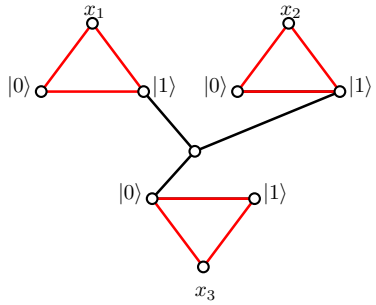
$(\|101\rangle - \|010\rangle)(\langle 101\| - \langle 010\|)$	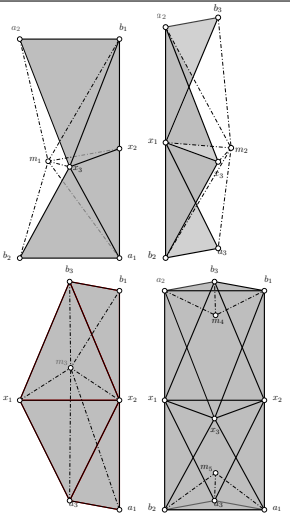	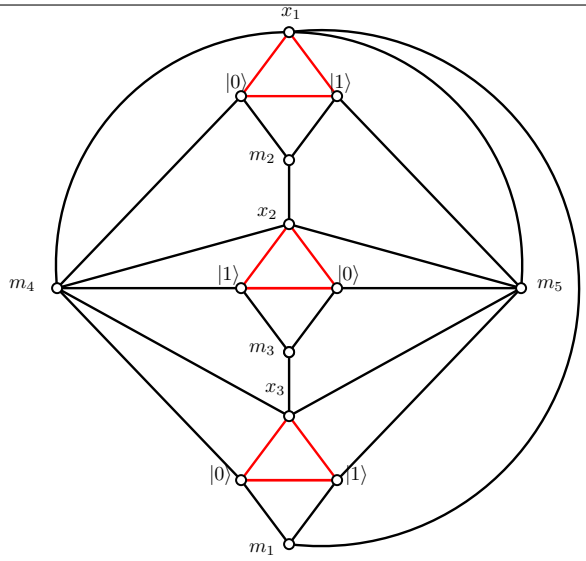

Table 1.3: Collection of gadgets for the 3-qubit projectors in the clock Hamiltonian of quantum 4-SAT. In order to aid readability for the entangled state we have shown the simplices connected to m_1, m_2 and m_3 on separate graphs, and shown how m_4 and m_5 are connected to the entire complex. We have also omitted the edges between mediators - these form a complete graph between the mediator vertices. The gadget which lifts the state $|011\rangle - |100\rangle$ is realised by permuting the order of the first and second triangles in the gadget which lifts the state $|101\rangle - |010\rangle$. The gadgets for propagation under the Pythagorean gate are more complicated, and are dealt with separately in subsection 1.3.1.5.

The final two mediators m_4 and m_5 are glued to the two missing faces:

$$[b_1 a_2 b_3 m_4]\,, \qquad [a_1 b_2 a_3 m_5]\,. \tag{1.3.24}$$

This covers all 14 faces of Σ_3. To fill in the spaces between the tetrahedra we simply connect all the mediators by edges. This defines additional tetrahedra which fill the void.

One can algebraically check that

$$|101\rangle - |010\rangle = \partial\,|\Psi\rangle\ , \tag{1.3.25}$$

where $|\Psi\rangle$ is the equal weight superposition of the 14 3-simplices presented in eq. (1.3.23) and eq. (1.3.24), along with the following 3-simplices involving 2 mediators:

$$\begin{gathered}
([a_2 x_3] + [x_3 b_2]) \wedge [m_1 m_2] \\
([b_3 x_1] + [x_1 a_3]) \wedge [m_2 m_3] \\
([x_2 b_1] + [a_1 x_2]) \wedge [m_1 m_3] \\
([b_1 a_2 m_1] + [a_2 b_3 m_2] + [b_3 b_1 m_3]) \wedge [m_4] \\
([b_2 a_1 m_1] + [a_3 b_2 m_2] + [a_1 a_3 m_3]) \wedge [m_5]
\end{gathered} \tag{1.3.26}$$

the following 3-simplices involving 3 mediators:

$$\begin{gathered}
([a_2 m_2 m_1] + [b_3 m_3 m_2] + [b_1 m_1 m_3]) \wedge [m_4] \\
([a_3 m_2 m_3] + [b_2 m_1 m_2] + [a_1 m_3 m_1]) \wedge [m_5]
\end{gathered} \tag{1.3.27}$$

and finally, two 3-simplices which just involve the mediators:

$$[m_2 m_1 m_3 m_5] + [m_1 m_2 m_3 m_4] \tag{1.3.28}$$

Checking that the state given above satisfies $|101\rangle - |010\rangle = \partial\Psi$ is a straightforward (if rather tedious) calculation. However actually finding the state for this gadget was more involved. In the case of the 2 qubit, and classical 3 qubit, gadgets, we could find Φ satisfying $c = \partial(\Phi)$ simply by looking at the simplicial complex - this was possible because the mediators introduced in those gadgets didn't introduce any higher dimensional simplices into the complex, and the filled in cycle was easy to visualise. As the cycle, c, to fill in increases in size and complexity this becomes increasingly difficult, and instead we solve a set of equations to demonstrate both that there exists a Φ satisfying $c = \partial(\Phi)$, and that c is the only cycle that can be written in this way. This is the same set of equations we use to demonstrate that all the gadgets we use fill in only the desired state, and not any extra ones. Details of the calculations are given in subsection 1.3.1.7. In the same section we also demonstrate that no new holes are introduced by this gadget, and therefore we have not added any unwanted elements to H_2.

1.3.1.4 General approach

The procedures described above depend on the details of the cycle to be filled in. We now describe a general procedure. The procedure we describe is far from optimal, in that it will generically required a greater number of mediators and edges that are minimally required, but it has the advantage of being of general applicability and no particular insights into the details of the cycle being filled in are required. We don't prove that this procedure works in general (as a procedure for general cycles is not needed for our result). However, we include this high level description as this is the procedure we will use to fill in the cycles generated by propagation under the

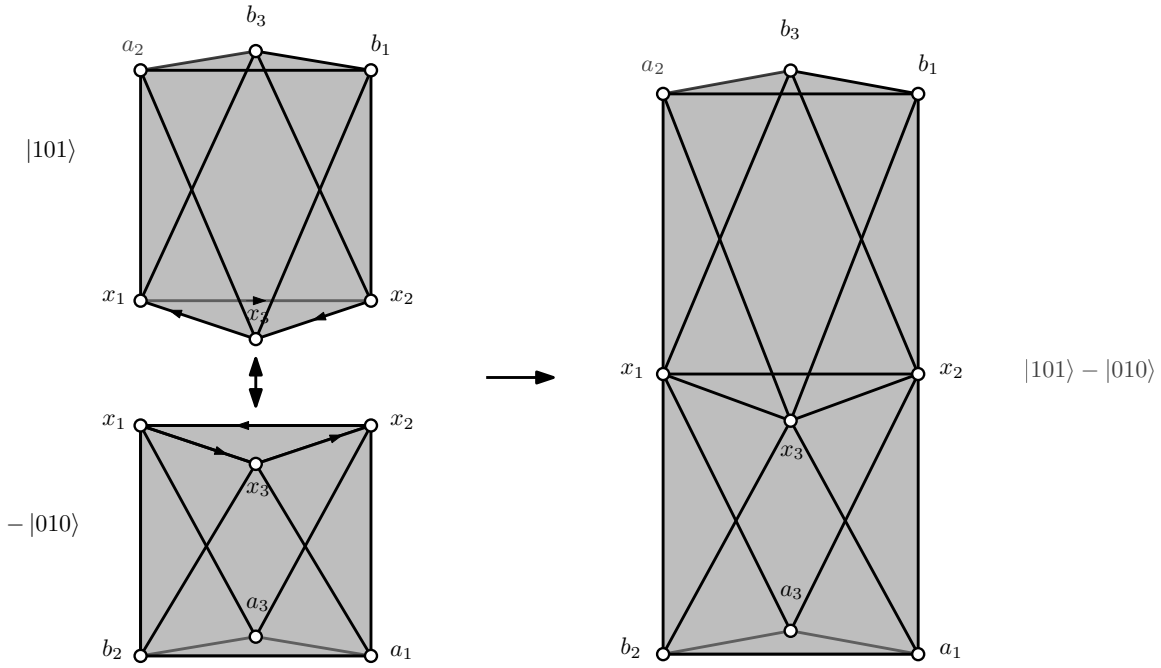

Figure 1.7: Combining the two 2-dimensional voids $|101\rangle$ and $-|010\rangle$ into the 2-dimensional void bounded by the entangled state $|101\rangle - |010\rangle$. Note that the face $[x_1x_2x_3]$ is common to both cycles but comes with opposite orientations and thus cancels in the superposition, leaving only *one* void to be filled. Additional vertices and edges which are not relevant have been omitted for clarity.

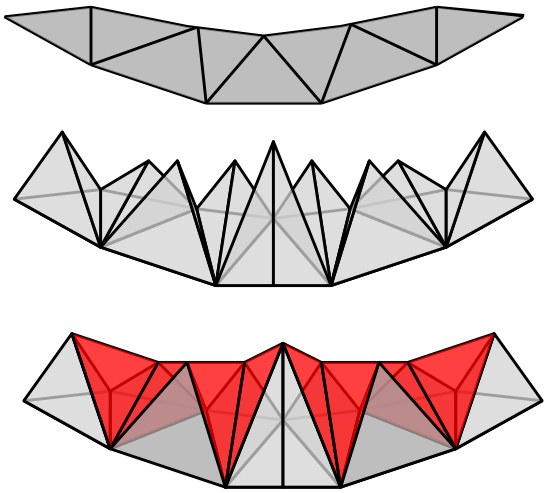

Figure 1.8: General approach to filling a 2-dimensional cycle. The first picture is a part of a 2-dimensional closed surface. For each face $[f_i]$ in the surface we add include a mediator m_i and connect the mediator to all the vertices of $[f_i]$ to form a solid tetrahedron $[f_i m_i]$. This leaves some empty voids in between the tetrahedra, which are filled by connecting mediators whose corresponding faces share an edge.This leads to a closed shell with an inner void. Finally, choosing one of the mediators to connect to all others fills the void and we obtain a three-dimensional space whose boundary is $\sum_i [f_i]$, as desired.

Pythagorean gate in the next section. The Pythagorean gadgets are the most technically involved gadgets in the proof, and it is useful to understand the high level process before delving into the details of the specific gadget.

Consider an n-dimensional cycle $|s\rangle$ defined by a set of n-simplices $[f_i]$,

$$|s\rangle = \sum_i [f_i] \,. \tag{1.3.29}$$

To fill in this (and only this) cycle we proceed as follows. For concreteness, consider a 2-cycle. Then, for every face $[f_i]$ we introduce a mediator m_i and add the solid tetrahedron $[f_i m_i]$ to the simplicial complex. This partially fills in the inner space but leaves some empty 3-dimensional "wedges" between the tetrahedra corresponding to neighboring faces (second picture in Fig. 1.8). We can fill these in by connecting the mediators m_i and m_j with the edge e_{ij} that is common among faces $[f_i]$ and $[f_j]$. This generates a "shell" whose outer boundary is the surface we wish to fill (see the third picture in Fig. 1.8), leaving only an inner empty void. To fill in this inner void we add one final mediator vertex, which is connected to all other mediator vertices. Algebraically, this amounts to the statement that there exist a 3-chain $|V\rangle$ such that

$$|s\rangle = \partial\,|V\rangle \sim 0 \,. \tag{1.3.30}$$

Furthermore $|s\rangle$ is the *only* cycle rendered trivial in homology by this procedure. (If one wishes to fill in several cycles the procedure must be carried out for each one).

1.3.1.5 The 3-qubit Pythagorean gadget

This is the most technically challenging gate. The states to be lifted are

$$|\psi_{Pyth.}\rangle = \frac{1}{5\sqrt{2}}\left(-5\,|011\rangle + 4\,|100\rangle + 3\,|101\rangle\right) , \qquad |\psi_{Pyth.}\rangle = \frac{1}{5\sqrt{2}}\left(-5\,|010\rangle + 3\,|100\rangle - 4\,|101\rangle\right) . \tag{1.3.31}$$

The complication stems mainly from the fact that there are three distinct computational cycles entering each entering 3, 4, or 5 times (up until now we only had computational cycles appearing with coefficients ± 1). For concreteness we focus on the first state in (1.3.31). The three computational cycles are explicitly,

$$\begin{aligned}
A = |011\rangle &= [x_1x_2x_3] + [x_1b_3x_2] + [b_2x_1x_3] + [x_1b_2b_3] + [a_1x_3x_2] + [a_1x_2b_3] + [a_1b_2x_3] + [b_2a_1b_3] \,, \\
B = |100\rangle &= [x_1x_2x_3] + [x_1a_3x_2] + [a_2x_1x_3] + [x_1a_2a_3] + [b_1x_3x_2] + [b_1x_2a_3] + [b_1a_2x_3] + [a_2b_1a_3] \,, \\
C = |101\rangle &= [x_1x_2x_3] + [x_1b_3x_2] + [a_2x_1x_3] + [x_1a_2b_3] + [b_1x_3x_2] + [b_1x_2b_3] + [b_1a_2x_3] + [a_2b_1b_3] \,.
\end{aligned} \tag{1.3.32}$$

The strategy is then to consider copies of each $-A$, B, and C cycles separately and glue them appropriately to obtain the cycle $|\psi_{Pyth.}\rangle$. To do so we describe a procedure which we term "simplicial surgery," in which we cut each of these cycles in a certain way (described below) and glue them along the cuts to form the closed surface $|s\rangle = |\psi_{Pyth.}\rangle$. Once $|\psi_{Pyth.}\rangle$ is obtained this way, we fill it in by tetrahedra by the general method described in subsection 1.3.1.5. The procedure for the second state in (1.3.31) is similar and we provide the details in subsection 1.3.1.6.

To understand how to precisely glue these cycles, note that B and C have the two edges $[b_1x_2]$ and $[b_1a_2]$ in common. We will glue together the B and C cycles by cutting open the cycles along this shared edge, and gluing together the cycles along the open 1-cycle this creates. Take four copies of B and three copies C. Then, in each cycle create a duplicate vertex b_1' and include the edges $[b_1'x_2]$ and $[b_1'a_2]$. This leads to cycles with slits cut into them (see Fig. 1.9). Now we glue together the cycles by identifying the a_2 and x_2 vertices from the different cycles, and identifying b_1' from cycle i with b_1 from cycle $i+1$.

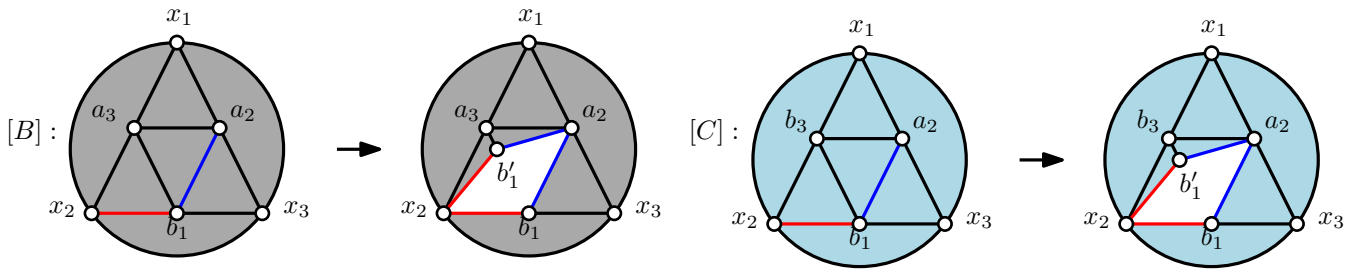

Figure 1.9: The $[B]$ and $[C]$ cycles are cut open by cutting a slit along $[x_2b_1]+[b_1a_2]$ by duplicating the middle point b_1. Here we have omitted vertices and edges to keep the pictures clear but one should bear in mind that before performing the cut each is a closed 2-cycle, homeomorphic to S^2. Then, the open cycles are connected with each other by gluing through the common one-cycles $[x_2b_1]+[b_1a_2]+[a_2b_1']+[b_1'x_2]$, ensuring the orientation is consistent, and attaching the $[A]$-cycles by deleting the common face $[x_1x_2x_3]$. The resulting space, $A_5B_4C_3$ is a closed surface composed of the $[B]$ and $[C]$ cycles with the five $[A]$-cycles attached, as shown in Fig. 1.10. As a whole, the space $A_5B_4C_3$ is homeomorphic to S^2 and it is this topological S^2 which we wish to fill.

We then attach to this the five A cycles. This step is more straightforward since the A cycles are added with the opposite orientation to the B and C cycles. This means that when we are adding the cycles the common face $[x_1x_2x_3]$ cancels out and we can glue the cycles along this face. When adding an A cycle to a B cycle this simply amounts to identifying the x_1, x_2 and x_3 vertices from the A cycle with that of the B cycle, and adding the edges of the A cycle in the appropriate orientation. When adding the A cycles to the C cycles they also share the common face $x_1b_3x_2$, so the x_1, x_2, x_3 and b_3 faces from the A cycle are identified with those of the C cycle, and again the edges of the A cycle are added in the appropriate orientation. This leads to the closed surface $A_5B_4C_3$ shown in Fig. 1.10, which is bounded by $8\times 2+7\times 4+6\times 6=80$ faces, which we denote by $[f_i]$.[12] The resulting surface is homeomorphic to S^2. To fill this surface in we follow the general procedure from the previous section. For each face composing the surface we introduce a mediator vertex m_i and connect each to all the vertices of the corresponding $[f_i]$, forming a solid tetrahedron $[f_i\, m_i]$.

This introduces 80 mediator vertices which partially fill in the cycle defined by $|\psi_{Pyth.}\rangle$, but leave some gaps. We then introduce an edge between two mediators if the faces they are connected to share an edge or a vertex, which starts filling the gaps. Finally we add a last mediator vertex, and connect it to the other 80. This fills in all gaps in the surface, so that the cycle defined by $|\psi_{Pyth.}\rangle$ is closed.

We then identify all the copies of the original vertices with themselves, leaving the connections between the original vertices and the mediators unchanged. This leads to a simplicial complex Σ_3' consisting of 90 0-simplices, 581 1-simplices, 1049 2-simplices, 597 3-simplices, and 29 4-simplices. The Euler characteristic is $1-90+581-1049+579-29=-7$, consistent with $H_2(\Sigma_3')=(\mathbb{C})^7$.

The graph gadget G_3' is shown in Fig. 1.11. The resulting graph has $9+81=90$ vertices, 3424 edges and maximum vertex degree $\delta=81$. The explicit procedure for constructing this gadget is carried out step-by-step in the attached Mathematica file [15]. Details of the calculations carried out to show that this gadget closes the cycle associated to $|\psi_{Pyth.}\rangle$ and only this cycle are given in subsection 1.3.1.7 (where we also demonstrate that

[12] The two lots of 8 faces come from the B cycles which aren't attached to any A cycle. The four lots of 7 faces come from the two sets of A and B cycles that are attached to each other, since the common face $[x_1x_2x_3]$ has cancelled out. The six lots of six faces comes from the 3 sets of A and C cycles that are attached together since the common faces $[x_1x_2x_3]$ and $[x_1b_3x_2]$ have cancelled out.

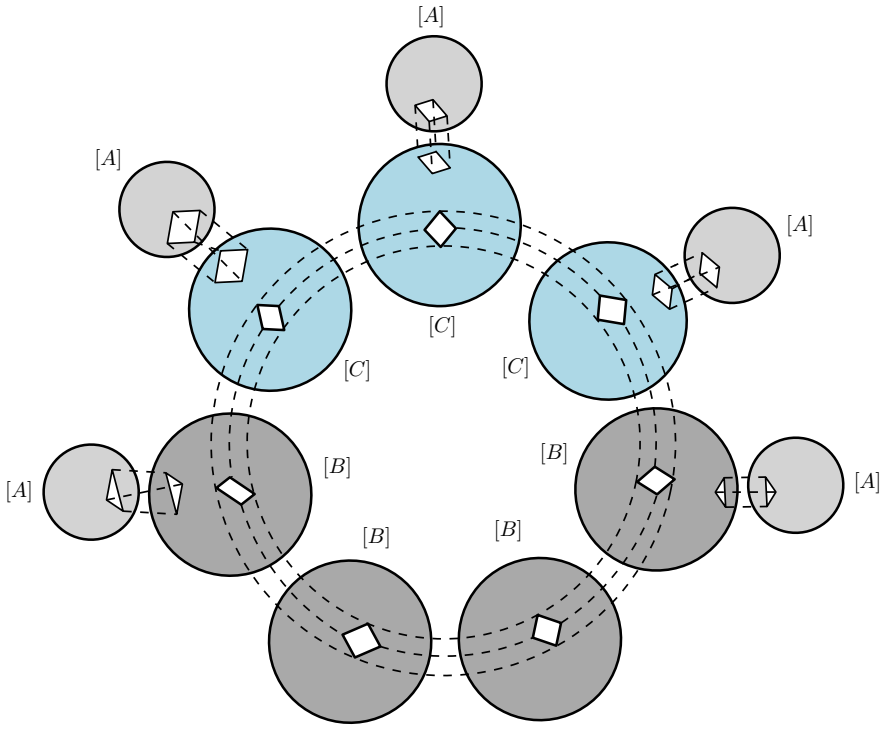

Figure 1.10: The Pythagorean cycle to be filled in is obtained by attaching five copies of $[A]$ which corresponds to the cycle $|011\rangle$ with that face $[x_1x_2x_3]$ missing.

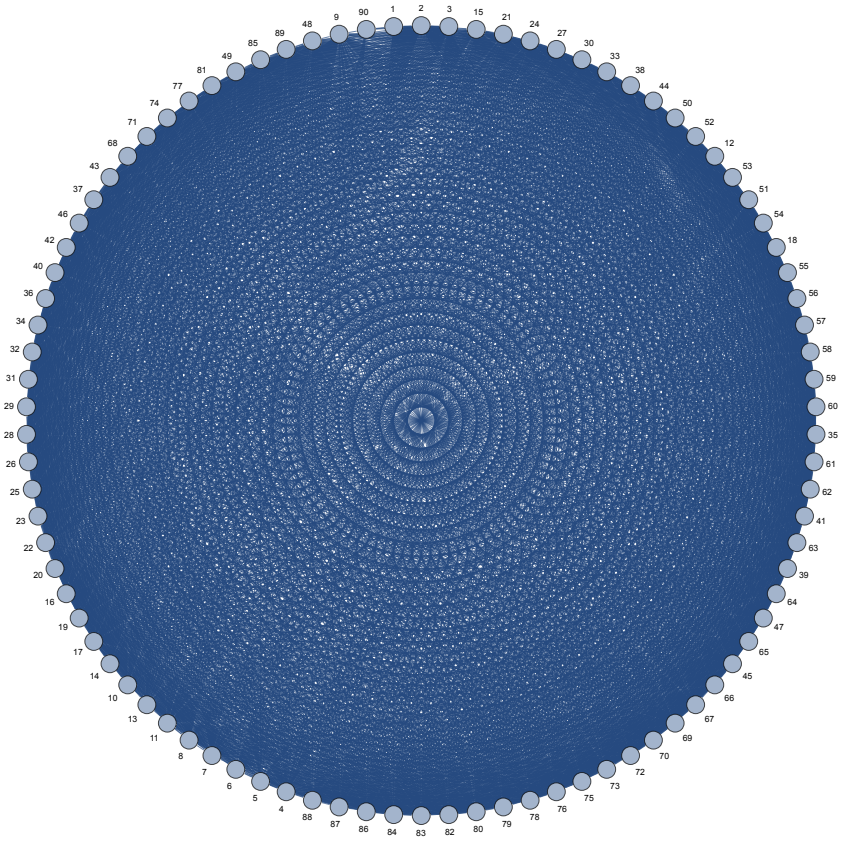

Figure 1.11: The Pythagorean gadget graph $G_{Pyth.}$ The maximum degree of $G_{Pyth.}$ is $\delta = 81$.

no new holes are introduced by this gadget). A similar process works for the other Pythagorean gadget, details can be found in subsection 1.3.1.6.

We point out that this technique of gluing faces together can be applied in general to any state of the form

$$|\psi\rangle = \sum_i n_i |e_i\rangle \ , \tag{1.3.33}$$

where the $|e_i\rangle$ are the computational cycles and the $n_i \in \mathbb{Z}$ are *integer* coefficients. The method does not apply, however, if the coefficients in (1.3.33) are general complex numbers. Although such states are well defined as abstract elements of the chain complex $C(\Sigma)$, they cannot be interpreted geometrically as cycles in a *simplicial* complex and our procedure for lifting such states in terms of adding discrete data such as mediator vertices and edges is not available. This is the reason we consider the non-standard universal gate set in our definition of QMA_1, which involves only rational coefficients and requires to lift the with states with integer coefficients (1.3.31). As long as the coefficients in the universal gate set are rational, however, this method carries through and therefore the homology problem is QMA_1-hard for all such definitions of QMA_1.

1.3.1.6 Geometric description of second Pythagorean gadget construction

The second Pythagorean gadget, to lift the state:

$$|\psi_{Pyth.}\rangle = \frac{1}{5\sqrt{2}} \left(-5\,|010\rangle + 3\,|100\rangle - 4\,|101\rangle\right) . \tag{1.3.34}$$

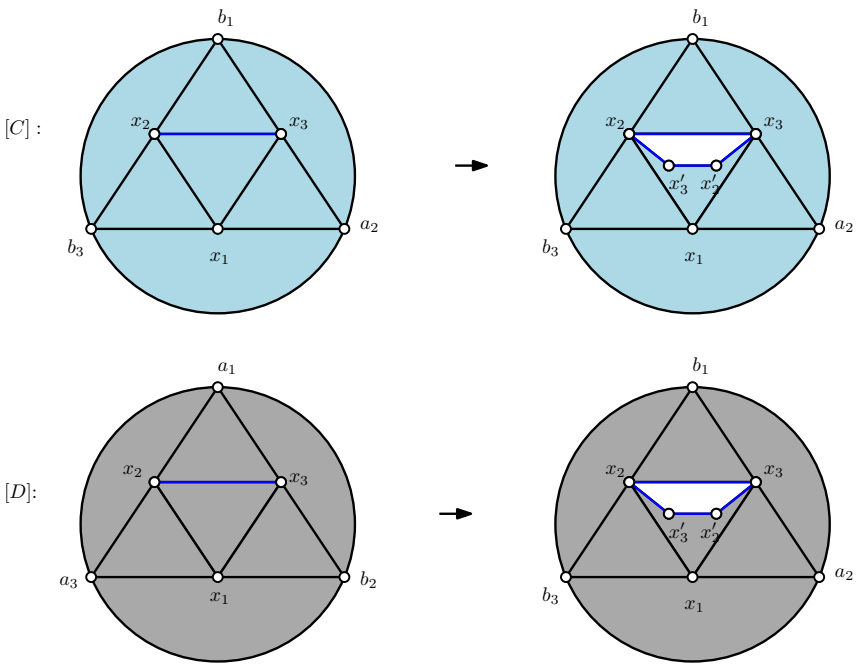

Figure 1.12: The $[C]$, $[D]$ and $[C+D-B]$ cycles are cut open by cutting a slit in the $[x_1x_2x_3]$ triangle by duplicating the points x_2 and x_3. Then, the open cycles are connected with each other by gluing through the common one-cycles $[x_2x_3]+[x_3x'_2]+[x'_2x'_3]+[x'_3x_2]$, ensuring the orientation is consistent. The $[C+D-B]$ cycle is cut open and glued together in the same way - the figure for that cycle is omitted as it is significantly more cluttered than the original cycles.

is designed in a similar way to the first Pythagorean gadget (outlined in subsection 1.3.1.5) but there are some modifications required.

Writing each computational cycle involved explicitly we have

$$\begin{aligned} B = |100\rangle &= [x_1x_2x_3]+[x_1a_3x_2]+[a_2x_1x_3]+[x_1a_2a_3]+[b_1x_3x_2]+[b_1x_2a_3]+[b_1a_2x_3]+[a_2b_1a_3]\,, \\ C = |101\rangle &= [x_1x_2x_3]+[x_1b_3x_2]+[a_2x_1x_3]+[x_1a_2b_3]+[b_1x_3x_2]+[b_1x_2b_3]+[b_1a_2x_3]+[a_2b_1b_3]\,. \\ D = |010\rangle &= [x_1x_2x_3]+[x_1a_3x_2]+[b_2x_1x_3]+[x_1b_2a_3]+[a_1x_3x_2]+[a_1x_2a_3]+[a_1b_2x_3]+[b_2a_1a_3]\,, \end{aligned} \tag{1.3.35}$$

We now need to carry out “simplicial surgery" on these cycles to generate $|\psi_{Pyth.}\rangle$.

Applying exactly the same process as in subsection 1.3.1.5 quickly runs into trouble. The C and D cycles only have three edges in common - $[x_1x_2]$, $[x_2x_3]$ and $[x_3x_1]$. But trying to glue along any two of these edges cannot work to construct the full cycle, since the cycle $C-B$ does not contain the edges $[x_3x_1]$ or $[x_2x_3]$ and the $D-B$ cycle does not include the edge $[x_1x_2]$. So if we glue together the C and D cycles and then try to subtract of the B cycles you will inevitably subtract off an edge that has been used to glue the cycles together.

To get around this we instead glue together three copies of the cycle $[C+D-B]$, one copy of the cycle C and two copies of the cycle D. Clearly this amounts to adding together the right number of copies of each cycle, but crucially these cycles all have the simplex $[x_1x_2x_3]$ in common. So we can glue along this simplex using the technique outlined in Fig. 1.12. We cut open the simplex by duplicating the vertices x_2 and x_3, and connecting up the vertices within cycles and between cycles to generate the necessary void.

This leads to a closed surface which is bounded by 67 faces. The surface is homeomorphic to S^2 and we fill it in using exactly the same procedure outlined in subsection 1.3.1.5.

This introduces 68 mediator vertices and leads to a simplicial complex Σ_3' consisting of 77 0-simplices, 489 1-simplices, 869 2-simplices, 462 3-simplices, and 13 4-simplices. The Euler characteristic is $1-77+489-869+462-13=-7$, consistent with $H_2(\Sigma_3')=(\mathbb{C})^7$.

As in subsection 1.3.1.5, to construct the graph we take the graph complement of the 1-skeleton of the resulting simplicial complex. This gives a graph on 77 vertices, with 2437 edges and maximum vertex degree $\delta=77$.

The explicit procedure for constructing this gadget is carried out step-by-step in the attached Mathematica file [15]. Details of the calculations carried out to show that this gadget closes the cycle associated to $|\psi_{Pyth.}\rangle$ and only this cycle are given in subsection 1.3.1.7.

1.3.1.7 Demonstrating that the gadgets fill in exactly one state and do not induce spurious homology classes

As outlined in subsection 1.3.1 the homology group of the clique complex of a graph consisting of n disconnected triangles is isomorphic to $\mathbb{C}^{\otimes n}$. That means that given a basis $v_i^{(n)}$ for $\mathbb{C}^{\otimes n}$ we will find that for all i: $\partial_n v_i^{(n)}=0$ and there does not exist any state $c^{(n+1)}$ satisfying:

$$\partial_{n+1}c^{(n+1)}=v_i^{(n)} \tag{1.3.36}$$

Analytically, 'filling in cycles' in the clique complex corresponds to breaking the second of these conditions. The states we are lifting are still cycles, so the first condition still holds. But by 'filling in the cycle' we are constructing a state which the cycle is a boundary of, and hence there now does exist a state $c^{(n+1)}$ satisfying eq. (1.3.36).

Therefore, to check that for each of the gadgets we have constructed we lift the desired state, and only that state, we need to check that the only state for which eq. (1.3.36) has a solution is the state that we are intending to lift.

So, in Mathematica for a gadget acting on n qubits we solve the equation:

$$\sum_{i,j}\left(k_i\left|e_i^{(n)}\right\rangle-b_j\partial_{n+1}\left|e_j^{(n+1)}\right\rangle\right)=0 \tag{1.3.37}$$

for k_i where $\left|e_j^{(x)}\right\rangle$ denotes the j^{th} independent set of size x in the graph. For all the gadgets presented in the paper, we find that (up to an irrelevant global phase) the only state satisfying eq. (1.3.37) is the intended state.

The calculations for all the gadgets are presented in the attached Mathematica file [15].

We also note that it can be seen straightforwardly that our gadgets do not induce spurious homology classes (i.e. they do not create any new holes in the independence complex). For individual gadgets this can be seen by studying the geometry:

- In the case of the 2 qubit gadgets this is straightforward - simply by inspecting the complexes in Table 2 it can be seen that every cycle that is induced by the mediators is a boundary of a triangle / collection of triangles, and therefore there are no new homology classes.
- For the CNOT gadget introduced on page 17, this cannot be visualized as it is a higher-dimensional object, but it can nonetheless be understood geometrically. First consider adding the mediators and their connections to the original vertices (but without adding the connections between the mediators). All we have added at this stage is a solid tetrahedron. Therefore there are no new homology classes at this stage since every cycle involving one of the mediators can be continuously deformed either to a point or to one of the previously

existing cycles. When we carry out the next step and fill in the original hole we do so by adding a solid tetrahedron between the mediators - so again every new cycle can be continuously deformed either to a point or to one of the previously existing cycles, and thus there are no new homology classes.

- The same reasoning applies to the Pythagorean gadget - every time an edge is added between a mediator and any other vertex this edge forms part of a solid tetrahedron, and therefore cannot induce any new homology classes, as any new cycles can be continuously deformed to either a point or to one of the previously existing cycles.

When we come to combine gadgets together we have to consider adding projectors on overlapping qubits, tensoring on classical projectors, and tensoring on identity:

- When adding projectors Π_1 and Π_2 on overlapping qubits there are no edges in the clique complex between mediators arising from Π_1 and those arising from Π_2 so there are no cycles involving mediators from both gadgets that cannot be continuously deformed into cycles arising from just one projector, and therefore there are no new homology classes.
- When tensoring on classical projectors or the identity we are again adding solid simplices between the mediators of the classical projector and the original vertices / mediators from the entangled projector, so every new cycle can be continuously deformed to either a point or a previously existing cycle.

1.3.1.8 Combining gadgets together

The projectors needed for the various Hamiltonian terms in Table 1.1 involve the tensor product of the projectors just discussed. Furthermore, in order to construct the full Hamiltonian we will need to take the sum of all these terms. Thus, the final ingredient needed for the reduction from quantum 4-SAT to the homology problem is to understand how to take tensor products and sums of the gadgets just described. Luckily, this is straightforward.

Adding projectors. When adding two projectors the states 'lifted' by the individual projectors are still lifted. Thus, given two projectors Π_1 and Π_2 the gadget for the sum

$$\Pi = \Pi_1 + \Pi_2 \tag{1.3.38}$$

is obtained by independently filling in the corresponding cycles in Σ_n for each projector. If any qubits are simultaneously acted upon by both projectors then we need to overlap the gadgets, while taking care not to render any other states equivalent in the homology. The general procedure for doing this for a pair of projectors Π_1 (implemented by the graph G_1) and Π_2 (implented by the graph G_2) which act on a total of n qubits is:

1. Start constructing the graph G_{12} with n triangles.
2. If there are any mediators in the graphs G_1 and G_2 which connect to exactly the same set of qubit vertices in the two graphs, add this mediator and the corresponding connections to the graph G_{12} *once*. Label this set of mediator vertices by $\{m_{12}\}$.
3. Take the remaining mediators from the graph G_1 and add them, and their corresponding connections, to the graph G_{12}, and label this set of mediator vertices by $\{m_1\}$. Do the same for G_2, and label this set of mediator vertices by $\{m_2\}$.
4. Add connections from every vertex in the set $\{m_1\}$ to every vertex in the set $\{m_2\}$.

The final step in this procedure may seem superfluous. Indeed, constructing the gadgets without this step does lead to the desired states being lifted, but it can also render some ground states equivalent in the homology.

If this occurs then the homology group of the corresponding graph is no longer isomorphic to the ground state of the desired projector. Adding connections between the mediators arising from the different projectors prevents this from happening, preserving the isomorphism between the homology group and the ground state.

We will use the gadgets for lifting $|\phi_1\rangle = |00\rangle - |11\rangle$ and $|\phi_2\rangle = |01\rangle - |10\rangle$ as an illustrative example to explain this point.

Implementing the projector $|\phi_1\rangle\langle\phi_1| + |\phi_2\rangle\langle\phi_2|$ requires filling in the cycles:

$$\phi_1 = [x_2\, a_1] + [a_1\, a_2] + [a_2\, x_1] + [x_1\, b_2] + [b_2\, b_1] + [b_1\, x_2]\,, \tag{1.3.39}$$

$$\phi_2 = [x_2\, a_1] + [a_1\, b_2] + [b_2\, x_1] + [x_1\, a_2] + [a_2\, b_1] + [b_1\, x_2] \tag{1.3.40}$$

It can be straightforwardly checked that the graph resulting from applying steps 1-3 from the process for adding projectors in subsection 1.3.1.8 to the graphs for the individual projectors from Table 1.2 does fill in the required cycles. However, a simple calculation demonstrates that this graph has Euler Characteristic 1 - this implies that the homology group H_2 only contains one element. It therefore cannot be isomorphic to the ground state of $|\phi_1\rangle\langle\phi_1| + |\phi_2\rangle\langle\phi_2|$, which is dimension two.

This issue arises because the mediators added to the graph have caused two previously independent homology classes to be homologous to one another.

To see why that has happened we will consider the states $|\phi_3\rangle = |00\rangle + |11\rangle$ and $|\phi_4\rangle = |01\rangle + |10\rangle$ - clearly these states span the ground state of the projector that we want to implement, and in the original gadgets they form distinct members of the homology.

To see that they are distinct members of the homology in the original projectors we note that:

$$\phi_3 = [x_2\, a_1] + [a_1\, a_2] + [a_2\, x_1] + [x_1\, x_2] + [x_2\, b_1] + [b_1\, b_2] + [b_2\, x_1] + [x_1\, x_2]\,, \tag{1.3.41}$$

$$\phi_4 = [x_2\, a_1] + [a_1\, b_2] + [b_2\, x_1] + [x_1\, x_2] + [x_2\, b_1] + [b_1\, a_2] + [a_2\, x_1] + [x_1\, x_2] \tag{1.3.42}$$

And therefore:

$$\phi_3 - \phi_4 = [a_1\, a_2] + [a_2\, b_1] + [b_1\, b_2] + [b_2\, a_1] \tag{1.3.43}$$

It can be checked that in the original gadgets there is no 3-cycle for which the cycle $\phi_3 - \phi_4$ is a boundary, and therefore the two cycles are not homologous to one another. However, it can be seen from Fig. 1.13 that if we try to combine the projectors $|\phi_1\rangle\langle\phi_1|$ and $|\phi_2\rangle\langle\phi_2|$ without connecting the mediators in the graph, then in the independence complex we have constructed a 3-cycle which $\phi_3 - \phi_4$ is a boundary of, and so the two cycles are homologous to each other.

By connecting the mediators from the set $\{m_1\}$ with the mediators from the set $\{m_2\}$ in the graph, we remove the connections between the mediators in the independence complex - and the two states ϕ_3 and ϕ_4 are again members of distinct homology classes, as required.

It is worth noting that connecting the mediators isn't always necessary - for particularly simple gadgets (e.g. two classical gadgets) this issue doesn't arise. Moreover, in cases where the gadgets overlap on some, but not all, qubits it is generally possible to construct the correct gadget by connecting some, but not all, mediators from the different gadgets. However, connecting all the mediators from the different gadgets will always work. So, for clarity we assume that for all gadgets on overlapping sets of qubits we connect all the mediator vertices arising from one gadget with all the mediator vertices arising from the other gadget.

(a) Independence complex arising from trying to add projec- (b) Independence complex arising from correctly adding pro-
tors without connecting the mediators together in the graph. jectors (connecting the mediators together in the graph.)

Figure 1.13: The independence complexes that arise from adding projectors together without (Fig. 1.13a) and with (Fig. 1.13b) connections between the mediators from different gadgets in the graph. In both figures the un-primed mediator vertices are those arising from the gadget for lifting ϕ_1, while the primed mediator vertices are those arising from the gadget for lifting ϕ_2. In both cases superfluous vertices and edges have been omitted from the figure for clarity.

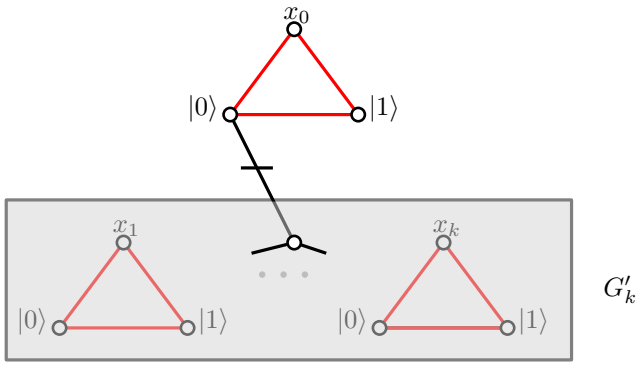

Figure 1.14: The qubit 0 at the top realizes the 1-qubit projector $|1\rangle\langle 1|$ and the bottom gadget G_k' implements $\Pi^{(k)}$. Connecting them as in the figure implements the $(k+1)$-qubit projector $\Pi^{(k+1)} = |1\rangle\langle 1| \otimes \Pi^{(k)}$.

Tensoring projectors. A number of tensor products between entangling projectors and classical projectors appear in Table 1.1. Consider a $(k+1)$-qubit projector of the form

$$\Pi^{(k+1)} = |1\rangle\langle 1| \otimes \Pi^{(k)}\,, \tag{1.3.44}$$

where $\Pi^{(k)}$ is a k-qubit projector and the identity operator is understood to be acting on the remaining qubits. If the first qubit above is in the state $|0\rangle$, any configuration of the remaining k qubits is in the kernel of $\Pi^{(k+1)}$. If instead it is in the state $|1\rangle$ this forces the k qubits to be in the kernel of $\Pi^{(k)}$. We wish to understand how to reproduce this in terms of the graph gadgets for $|1\rangle\langle 1|$ and $\Pi^{(k)}$. For clarity we consider an explicit example, but the logic can be applied to any such gadget. The case we will consider is the gadget for lifting the state $|1\rangle(|01\rangle - |10\rangle)$. The cycle that must be filled in order to lift the state $|01\rangle - |10\rangle$ is given by:

$$|01\rangle - |10\rangle = [x_1a_2] + [a_2b_1] + [b_1x_2] + [x_2a_1] + [a_1b_2] + [b_2x_1]\,. \tag{1.3.45}$$

Tensoring on the state $|1\rangle = [x_3] - [b_3]$ is equivalent to taking the wedge product $(|01\rangle - |10\rangle)|1\rangle = ([x_1a_2] + [a_2b_1] + [b_1x_2] + [x_2a_1] + [a_1b_2] + [b_2x_1]) \wedge ([x_3] - [b_3])$. Recall that when we lifted the state $|01\rangle - |10\rangle$ we filled the 1-cycle defined by the edges given in (1.3.45). To lift $|1\rangle(|01\rangle - |10\rangle)$ we clearly need to fill in a 2-cycle, and we can see the form of that 2-cycle by considering the wedge product above. For each 1-simplex in (1.3.45) the tensor product will give rise to two 2-simplices - one including the original two vertices and x_3, the other with the original two vertices and b_3 (with opposite orientations). Thus, the cycle for the state $(|01\rangle - |10\rangle)|1\rangle$ will involves 12 2-simplices which bound the original 1-cycle (see Fig. 1.15c).

It is straightforward to see that taking the independence complex which filled the 1-cycle for $|01\rangle - |10\rangle$, and adding edges between each mediator and x_3 and b_3 will fill the required 2-cycle. From this independence complex, $\sum_t$, we can construct the graph G_t - see Fig. 1.15d.

The same logic carries over to the other examples where we have an entangled projector tensored with a classical projector. In each case, the k-simplices bounding the original cycle become $k+1$-simplices bounding the new cycle, and adding edges in the independence complex between the existing mediators and the additional vertices bounding the new cycle is sufficient to fill the necessary void. In the graph this is equivalent to adding an edge between the vertex that does *not* bound the new cycle (i.e. the vertex a if the classical projector is $|1\rangle\langle 1|$ and the vertex b if the classical projector is $|0\rangle\langle 0|$). See Fig. 1.14.[13]

Tensoring on the identity If we were to apply the logic for adding and tensoring projectors to the case of tensoring on the identity it would appear that this is a complex task. We would need to first construct the 'identity projection' onto some set of qubits by adding together a number of classical projectors, then tensor this sum of projectors onto the relevant non-trivial projection.

Fortunately, we can take a short cut that avoids this complication. Consider a projector Π_i acting on some set of qubits $\{i_k\}$ with gadget given by the graph G_i. If we want to tensor this with the identity on qubit j in the graph we simply take the graph G_i and add a triangle to represent the qubit j which is disjoint from the rest of the graph.

To see why this is equivalent to tensoring on the identity acting on qubit j consider Fig. 1.15 again. In that figure we demonstrate how to tensor on the classical projector $|1\rangle\langle 1|$ to the entangled projector $(|0\rangle - |1\rangle)(\langle 0| - \langle 1|)$.

[13] For readers who have already covered the connection to supersymmetry in Section 2.1 the form of these tensor product gadgets can be checked very quickly. Clearly if the qubit with the classical projector acting on it is in the kernel of the classical projector then the mediators are forced to be empty by the hard core condition, and the homology is non-trivial regardless of the state of the remaining qubits. If the classical qubit is not in the kernel of the classical projector, then the remaining qubits are forced to be in the kernel of the entangled projector otherwise the mediators will have trivial homology, and by the tic-tac-toe lemma so will the overall state.

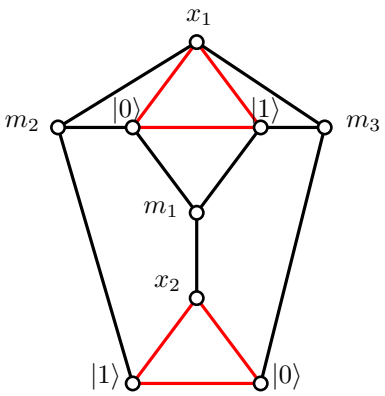

(a) Graph G to fill in the state $|01\rangle - |10\rangle$

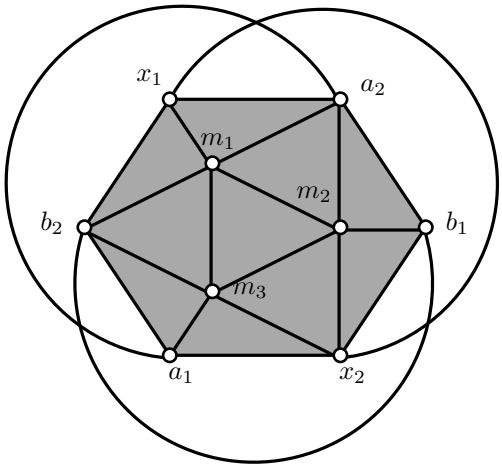

(b) Independence complex $\sum$ to lift the state $|01\rangle - |10\rangle$.

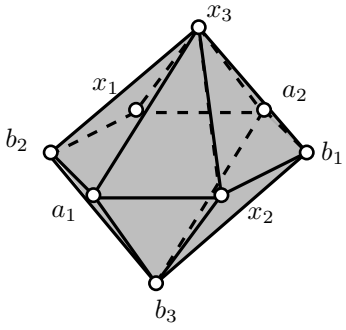

(c) To lift the state $|1\rangle(|01\rangle - |10\rangle)$ we need to fill in the 3-dimensional void shown in this figure. Irrelevant vertices and edges have been omitted for clarity.

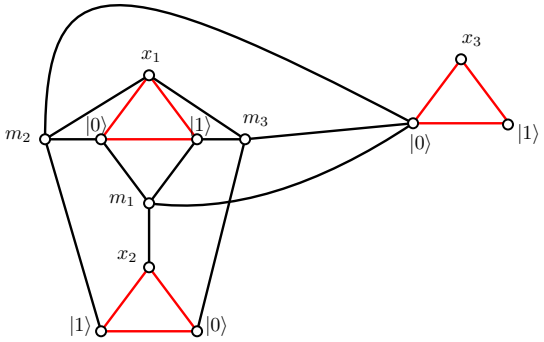

(d) Graph G_t to lift the state $|1\rangle(|01\rangle - |10\rangle)$.

Figure 1.15: Tensoring on a classical projector to an entangled one is equivalent to turning the k-simplices bounding the cycle from the original projector into $k+1$-simplices which bound the cycle we need to fill in for the new projector. This new void can be filled in by adding edges between the additional vertices bounding the cycle and all mediators from the original projector in the independence complex. In the graph this is equivalent to adding edges between the vertex *not* bounding the cycle and all the mediators.

To modify this gadget so that we were instead tensoring the entangled projector with the identity we need to also lift the state $|0\rangle(|0\rangle - |1\rangle)$. Examining Fig. 1.15d and Fig. 1.15c we see that removing the connections between the $|0\rangle$ vertex of qubit j and the mediators from the graph G_i will achieve this, since it will give rise to another filled cycle of the same form as that in Fig. 1.15c, while it won't change the original filled cycle.[14]

1.3.2 QMA_1-hardness

The homology problem for simplicial complexes, parameterised by an input type $\mathcal{I}$ was defined in [16]:

Definition 2 ($\textsc{Homology}_{\mathcal{I}}(K, l)$)
Input: A simplicial complex K represented as $\mathcal{I}$ and an integer l.
Problem: Output YES if the l^{th} homology group of K is non-trivial and NO otherwise.

In this section, we will prove that this problem is QMA_1-hard when the simplicial complex, K, is a clique complex $Cl(G)$ represented by G. As a stepping stone we consider the closely related problem when the complex is an independence complex $I(G)$ represented by G:

Lemma 1. $\textsc{Homology}_G(I(G), l)$ *is* QMA_1*-hard.*

Proof. We will demonstrate hardness by a reduction from an arbitrary problem in QMA_1 via the family of Hamiltonians used to show QMA_1-hardness of quantum 4-SAT in [8]. That is, for any Hamiltonian H_{Bravyi} which encodes a QMA_1-verification circuit via the techniques of [8], we will construct a graph G such that a particular homology group $H_l(d)$ of the independence complex $I(G)$ is non trivial iff there exists a satisfying assignment to the corresponding instance of quantum k-SAT. And therefore iff there exists a witness such that the QMA_1-verification circuit accepts with probability 1.

The ingredients for the construction are clear. Given an arbitrary problem in QMA_1 with input string x we construct a 5-local Hamiltonian H_{Bravyi} which encodes the problem and acts on $n = \mathsf{poly}(|x|)$ qubits.[15] We then construct a graph composed of n triangles (i.e. consisting of $3n$ vertices and $3n$ edges) and add mediators connecting triangles if they are jointly acted on by a projector in H_{Bravyi}. Where the form of the connections between triangles is given by the gadgets derived in the previous sections. We will demonstrate that the independence complex to the graph has non-trivial homology iff the encoded problem is a YES instance.

The input to the problem: H_{Bravyi} is made up of at most $\mathsf{poly}(n)$ rank-1 projectors. The gadgets we have constructed add $O(1)$ vertices to the graph for each projector. Therefore the final graph has $V = \mathsf{poly}(n)$, and the input size to the problem is $|V(G)|^2 = \mathsf{poly}(n) = \mathsf{poly}(x)$. The final part of the input to the problem is the integer l. Recall from the problem definition that the quantity of interest is the l^{th} homology group. For any fixed l this problem can be efficiently solved, however if l is allowed to grow with the input to the problem this is no longer the case. For our purposes, we will take $l = n - 1$.

Completeness: Given a YES instance of an arbitrary problem in QMA_1 there is a corresponding satisfying assignment to the instance of quantum 5-SAT that encodes the verification of this problem. Therefore there exists a state $|\Psi\rangle$ satisfying $H_{\text{Bravyi}}|\Psi\rangle = 0$. This state will correspond to an $(n-1)$-cycle, c, in the independence complex which is not a boundary - i.e. we have $\partial_{n-1}c = 0$ but $\nexists d$ such that $\partial_n d = c$. This follows since in the

[14] Again, readers who have already covered the material in Section 2.1 will immediately see that this is the correct procedure - in the Hamiltonian picture we are simply stating that acting with the identity on a set of qubits is equivalent to doing nothing.

[15] Recall, our Hamiltonian is 5-local instead of 4-local because our universal gate set includes a 3-local gate.

initial graph - consisting simply of n triangles - every element of the Hilbert space $(\mathbb{C}^2)^{\otimes n}$ is an $(n-1)$-cycle which is not a boundary. Adding the gadgets to build up a graph encoding the Hamiltonian H_{Bravyi} does not change the first equation, $\partial_{n-1}c = 0$ because no connections are added or removed between the initial $3n$ vertices by the gadgets, so the expression $\partial_{n-1}c$ is unchanged. Moreover, the gadgets fill in cycles iff they correspond to states that violate one of the projectors in H_{Bravyi}. But $|\Psi\rangle$ cannot violate any of the projectors in H_{Bravyi}, and as such the cycle corresponding to $|\Psi\rangle$ has not been filled in, and therefore we cannot write c as the boundary of some n-cycle. Therefore for YES instances the $(n-1)^{\text{th}}$ homology group of $I(G)$ is non-trivial.

Soundness: Given a NO instance of an arbitrary problem in QMA_1 the instance of quantum 5-SAT that encodes the problem has no satisfying assignments. Therefore every cycle which was not a boundary in the trivial graph (consisting of n disconnected triangles) has been filled in by the inclusion of the gadgets, and therefore the $(n-1)^{\text{th}}$ homology group of $I(G)$ is trivial.

Therefore, the $(n-1)^{\text{th}}$ homology group of $I(G)$ is non-trivial iff G encodes a YES instance of a QMA_1 problem. □

Theorem 1. HOMOLOGY$_G(Cl(G), l)$ *is* QMA_1*-hard.*

Proof. As noted in subsection 1.1.2 $Cl(G) = I(\overline{G})$. Moreover, given G the complement graph $\overline{G}$ can be computed in P. Therefore an arbitrary problem in QMA_1 can be reduced to HOMOLOGY$_G(Cl(G), l)$ via the reduction to HOMOLOGY$_G(I(G), l)$ given in Lemma 1. □

Furthermore, we note that the homology problem for clique complexes of graphs can be reduced to the homology problem for simplicial complexes given by vertices and minimal non-faces [16], and therefore we can derive the corollary:

Corollary 1. HOMOLOGY$_{\mathcal{I}}(K, l)$ *is* QMA_1*-hard when* $\mathcal{I}$ *is the vertices and minimal non-faces of* K*.*

1.3.3 QMA_1-hardness when restricted to clique-dense complexes

In [17] the hardness of HOMOLOGY$_G(Cl(G), l)$ for graphs which are *clique-dense* is considered, and is shown to be NP-hard. Where a graph is said to be clique dense if [18]:

$$\zeta_k^{-1} = \frac{\binom{n}{k+1}}{S_k} \in O(\mathsf{poly}(n)) \tag{1.3.46}$$

where S_k is the number of k-cliques in the graph. This regime is particularly interesting as it was believed to be the regime where quantum algorithms for homology would work best. As a corollary of our result we are able to lift the result from [17] to QMA_1-hardness:

Corollary 2. HOMOLOGY$_G(Cl(G), l)$ *remains* QMA_1*-hard when restricting to clique-dense graphs.*

In order to prove Corollary 2 we first need a side result about quantum k-SAT where the number of interactions each qubit is involved in is restricted.

1.3.3.1 Quantum (k, s)-SAT is QMA_1 hard

In quantum k-SAT the only constraint on the interaction graph is the number of qubits involved in each interaction (restricted to be no more than k). But obtaining clique-density when mapping to the homology problem requires also constraining the number of interactions each qubit is involved in. When we map to the homology

problem we will construct the mapping in terms of 'lifting' individual states, so in this section we will consider a rank m projector as the sum of m rank 1 projectors.To this end, we define a new problem:

Definition 3 (Quantum (k,s)-SAT)
Input: A set of k-local rank-1 projectors Π_S where S are possible subsets of $\{1,\ldots,n\}$ of cardinality k, such that each integer in the set $\{1,\cdots,n\}$ appears in no more than s projectors.
Promise: Either there exists a state $|\psi\rangle$ such that $\Pi_S|\psi\rangle = 0$ for all S or otherwise $\sum_S \langle\psi|\Pi_S|\psi\rangle \geq \epsilon$ for all $|\psi\rangle$, with $\epsilon > \frac{1}{\mathsf{poly}(n)}$.
Problem: Output YES if the former and NO if the latter.

We will show that quantum (k,s)-SAT with constant k,s is hard for QMA_1 using a technique from [46–48]. The idea is to show that any QMA_1-verification circuit can be efficiently mapped to a circuit where each qubit is involved in a constant number of gates. The mapping from circuit to Hamiltonian then preserves this property, so that each qubit is acted on by a fixed number of projectors, regardless of system size.

The utility of this technique will depend on the choice of universal gate set used to define QMA_1. It will work for any gate set where the SWAP gate can be implemented exactly. It is possible to implement the SWAP gate exactly using three CNOT gates, so crucially the hardness proof applies to our choice of gate set $\mathcal{G}$:

Lemma 2. *Quantum (k,s)-SAT is QMA_1-hard for $k \geq 5$ and $s \geq 32$.*

Proof. Consider a QMA_1-verification circuit consisting of n qubits which are acted on by a circuit $U = \Pi_{t=1}^{T} U_t$ (for $T = \mathsf{poly}(n)$) consisting of gates taken from the universal gate set $\mathcal{G}$.

We start by showing that this circuit can be mapped to one where each qubit is acted on by at most 3 gates, via a procedure initially used in [46–48] (see Fig. 1.16 for a graphical illustration of the process):

1. Place all the n qubits on a line, in some arbitrary ordering.
2. For each gate $U_i \in \{U_1,\cdots,U_T\}$, if U_i acts on a single qubit, or on adjacent do nothing. If U_i acts on a two or three qubits that are not adjacent then add a sequence of SWAP gates (implemented as three CNOT gates) before U_i, then reverse the SWAP gates after U_i. For each of the T gates in the circuit, this process adds at most $6n$ gates, so after this step the circuit consists of $T' = O(nT)$ nearest neighbour gates acting on a line of n qubits. We will denote this modified circuit by $U = \Pi_{t=1}^{T'} U'_t$
3. Take a $n \times T'$ grid of qubits. In each of the i^{th} column of the grid we will implement only the U'_i gate (which acts on adjacent) with all other qubits acted on by the identity gate. After implementing the gate U'_i on the i^{th} column we implement a row of SWAP gates between the i^{th} column and the $(i+1)^{th}$ column, so that the state of the qubits is mapped along the grid.

   In order to ensure that at each time step a constant number of qubits are acted on for the first time we implement the gates in the following order: in column i, start at the top and implement a series of identity gates until reaching the qubit(s) that U'_i acts on, then implement U'_i, then continue implementing identity gates on each qubit until we reach the bottom of the column. Then implement SWAP gates (via a sequence of three CNOT gates) between the qubits in column i and the corresponding qubits in column $i+1$ starting at the bottom of the column, and working up to the top.

   This circuit acts on $n' = nT' = \mathsf{poly}(n)$ qubits, and consists of $T_{\text{fin}} = 4(nT')^2 = \mathsf{poly}(n)$ gates (including identity gates), and each qubit in the circuit is involved in at most 7 gates (up to two SWAP gates each involving three CNOT gates, and one identity or non-trivial gate).

We will now use the clock construction from [8] to construct a mapping from our modified verification circuit to quantum (k, s)-SAT.

First consider the Hamiltonian H_{prop}. Each computational qubit is acted on by one projector of the form $H_{\text{prop,t}}$ for each gate it is involved in. Computational qubits are acted on by at most 7 gates, 6 of which are CNOT gates (rank 4). The final gate could be the identity gate or any other gate from $\mathcal{G}$ - so the corresponding projector has rank at most 8. So H_{prop} can be implemented by acting on each computational qubit with up to 32 rank one projectors. Each clock qubit is acted on by one projector of the form $H_{\text{prop,t}}$ (rank at most 4) and two projectors of the form $H'_{\text{prop,t}}$ (rank 1). So H_{prop} can be implemented by acting on each clock qubit with up to 6 rank one projectors.

The clock Hamiltonian only acts on the clock qubits. Each clock qubit is acted on by up to three rank 1 projectors, two rank 3 projectors, and one rank 4 projector. So H_{clock} can be implemented by acting on each clock qubit with up to 13 rank one projectors.

H_{out} acts on the final clock qubit and a single computational qubit in the last column of the grid with a single rank one projector.

The final piece of the puzzle is H_{in}. As set out in [8] H_{in} is a sum of rank one projectors, each one acting on the first clock qubit, and the non-witness computational qubits, i.e. all $q \in R_{\text{in}}$. However, implementing it in this fashion would lead to the first clock qubit being involved in a number of projectors which scales with the size of the problem since the number of $q \in R_{\text{in}}$ can scale with n. Following the same procedure as [47] we can get around this issue. At each time step in our modified circuit we only act with a single gate, so we don't need to initialise all the input qubits to zero when the clock is at zero. Instead we can initialise the input qubits to zero immediately before they are acted upon for the first time (possibly by an identity gate). So we replace the H_{in} from [8] by:

$$H_{\text{in}} = \sum_{q \in R_{\text{in}}, q \leq n} |1\rangle\langle 1|_q \otimes |a_1\rangle\langle a_1|_{c_{t_q}} \tag{1.3.47}$$

where c_{t_q} is the time at which qubit q is first acted on by a (possibly trivial) gate. We only need to add these terms for the first column of qubits, since the qubits in subsequent columns are 'dummy' qubits, and they are initialised by the SWAP gates.

The only computational qubits that will be acted on by H_{in} and H_{out} are in the first and last rows of the grid, so are acted on by at most 4 gates (since they are acted on by a single SWAP gate). So the qubits that are involved in the most projectors are computational qubits which are not in the first or last column of the grid. Therefore we can map our modified verification circuit to quantum (k, s)-SAT where $k = 5$ and $s = 32$.

□

For the universal gate set $\mathcal{G}$ used in this paper this proof only demonstrates hardness, since we have not shown that quantum $k-$SAT is contained within QMA_1 with this gate set. However, the proof of hardness could also be applied to the gate set $\mathcal{G}' = \{\text{CNOT}, \hat{H}, T\}$. In this case it is straightforward to see that all the projectors needed for the hardness construction have matrix elements in the computational basis of the form $\frac{1}{4}(a+ib+\sqrt{2}c+i\sqrt{2}d)$. It is shown in [9, Appendix A] that eigenvalues of projectors of this form can be measured exactly using the gate set $\mathcal{G}'$. Therefore, quantum $(k, s) -$ SAT with universal gate set $\mathcal{G}'$ where the set of allowed projectors $\mathcal{P}$ are all 4-local projectors with matrix elements in the computational basis of the form $\frac{1}{4}(a + ib + \sqrt{2}c + i\sqrt{2}d)$ is QMA_1-complete for $k \geq 4$ and $s \geq 28$ (the different constants are due $\mathcal{G}'$ not having a 3-qubit gate).

1.3.3.2 Clique homology restricted to clique-dense graphs QMA_1-hard

In this section we prove Corollary 2:

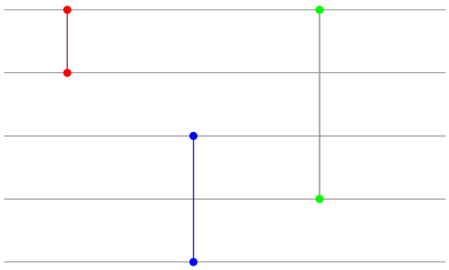

(a) The initial circuit we want to 'sparsify' - it consists of three two qubit gates.

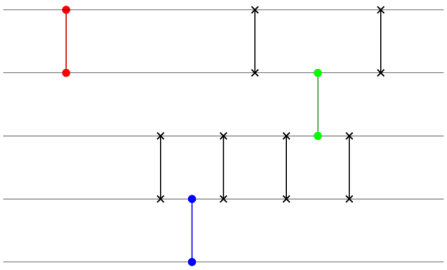

(b) The new circuit after the first step of the sparsification process - the SWAP gates ensure that all gates are nearest neighbour.

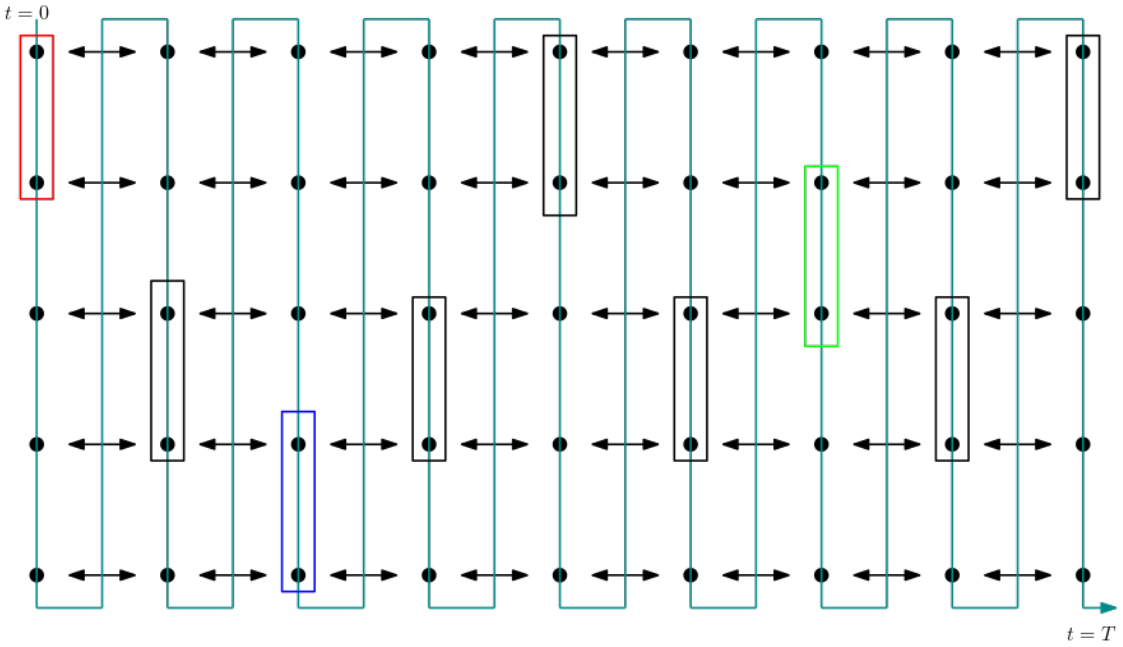

(c) The final step in the sparsification process. We now have a 7×5 grid of qubits, and the passage of time is denoted by the turquoise line, which starts at the top left and 'snakes' through the qubits. At each time step we either apply an identity gate to a particular qubit, a SWAP gate between qubits in different columns (denoted by an arrow), a SWAP gate between qubits in the same column (denoted by a black rectangle) or one of the original two qubit gates from Fig. 1.16a (denoted by red, blue and green boxes). In our construction the SWAP gates within the columns would actually be implemented as three CNOT gates acting in adjacent columns, however that detail is omitted from the figure for clarity.

Figure 1.16: A graphical representation of the 'sparsification' process applied in the proof of Lemma 2. This sparsification process has previously been used in [46–48].

Proof. We first show how to modify the reduction of Lemma 1 in such a way that the resulting graph G has constant degree. The only change is that we reduce from an arbitrary problem in QMA_1 via the family of Hamiltonians used to show QMA_1-hardness of quantum $(5, 32)$-SAT in the previous section. The projectors we need to implement are unchanged, so the proof follows by exactly the same logic as in Lemma 1.

The vertices of maximal degree in G will be those corresponding to mediators from a $H_{\text{prop,t}}(\text{CNOT})$ gadget acting on qubits which have a $H_{\text{prop,t}}(U_{Pyth.})$ and six $H_{\text{prop,t}}(\text{CNOT})$ projectors acting on them. The mediators in the $H_{\text{prop,t}}(\text{CNOT})$ gadget have maximum degree 11. When they are combined with the other gadgets acting on the same qubit, connections are added between these mediators and the 177 mediators from the two Pythagorean gadgets, and the 110 mediators from the other five CNOT gadgets, giving a total degree of 298. Therefore for the input graphs we are considering the degree is a constant $\delta = 298$. This results in an independence complex with $O(1)$-local boundary operator as claimed.

We have shown how to modify the reduction from Lemma 1 so that the maximum degree of any vertex in the graph G used to construct the independence complex $I(G)$ is $O(1)$. Therefore, when considering clique complexes the minimum degree of any vertex in the graph $\overline{G}$ is $O(n)$. By the clique-density theorem [19] we then have $S_k = O(n_k)$. Giving $\zeta_k^{-1} = O(1) \in \mathsf{poly}(n)$ as required. □

1.3.4 Containment in QMA with a suitable promise

To further pin down the complexity of the problem we need to consider the issue of a suitable promise. $\textsc{Homology}_{\mathcal{I}}(K, l)$ was presented as a decision problem - i.e. a promise problem with a vacuous promise. While it is known that there are problems in quantum complexity classes with vacuous promises (e.g. the *group non-membership* problem is known to be in QMA [20]) it is unlikely that a problem with a vacuous promise could be *complete* for QMA_1 [21]. Therefore we do not expect $\textsc{Homology}_{\mathcal{I}}(K, l)$ as stated to be contained in QMA_1.

From the statement of $\textsc{Homology}_{\mathcal{I}}(K, l)$ above it is not immediately obvious that it is possible to present it with a non-vacuous promise. A simplicial complex either has holes or doesn't, it appears to be a completely binary decision problem. However, it can be shown that the p^{th} homology group, $H_p(K)$ of a simplicial complex K is non-trivial iff the kernel of the combinatorial Laplacian $\mathcal{L}_p = \partial_p^\dagger \partial_p + \partial_{p+1} \partial_{p+1}^\dagger$ is non-empty (in fact, the p^{th} Betti number is given by the dimension of $\ker(\mathcal{L}_p)$, see e.g. [22]). This suggests a reformulation of $\textsc{Homology}_{\mathcal{I}}(K, l)$ with a suitable promise (this version first appeared in [23] for the general case of chain complexes, here for clarity we state it for simplicial complexes):

Definition 4 ($\textsc{Promise-Homology}_{\mathcal{I}}(K, p)$)
Input: A simplicial complex K represented as $\mathcal{I}$ and an integer p.
Promise: Either there exists a cycle $c \in C_p(K)$ such that $\mathcal{L}_p(c) = 0$ and hence $H_p(K) \neq 0$, or the smallest eigenvalue λ_p of $\mathcal{L}_p$ satisfies $\lambda_p \geq \epsilon$ with $\epsilon = \frac{1}{\mathsf{poly}(|\mathcal{I}|)}$
Problem: Output YES if the former and NO if the latter.

With this we can demonstrate that the homology problem for clique complexes (with a suitable promise) satisfying certain constraints lies in QMA:

Theorem 2. $\textsc{Promise-Homology}$ *for clique complexes $Cl(G)$ where the graph G is given as input is contained in* QMA *provided that G is clique dense.*

Proof. This follows from [23, Theorem 4] and [23, Proposition 1], where the statement is shown for k-local or

sparse boundary operators acting on chain complexes, with the operator ∂ given as input.[16] The ∂ operator for a clique complex is always sparse [24], and restricting the set of inputs cannot take the problem outside of QMA. So provided it is possible to efficiently obtain a description of ∂ from the graph G the theorem holds. Sparse access to ∂ can be obtained efficiently from a description of G via the prescription given in [24].

□

Since the QMA_1-hardness result holds in the case of clique dense complexes, this suggests that the problem of determining whether the homology group of a clique complex is non-trivial may lie between QMA_1 and QMA. However care must be taken – we have not shown that the promise version of the homology problem is QMA_1-hard, or that the decision version of the problem is in QMA. So while we believe that a result along these lines is likely to hold, we cannot claim it yet.

1.3.5 The Betti number problem

The problem of interest in topological data analysis is typically calculating how many holes a clique complex has at dimension l - or determining the l^{th} *Betti number*. An immediate consequence of our QMA_1-hardness of the homology problem is the following:

Theorem 3. *Given a graph G on n vertices the problem of computing the l^{th} Betti number of its clique complex is #P-hard for $l = \Omega(n)$.*

Proof. To prove Theorem 1 we demonstrated how to construct a graph G such that the Betti number β_n is equal to the number of satisfying assignments to a quantum 5-SAT instance. The problem of counting satsifying assignments for quantum k-SAT is known to be #P-hard [23, 25].

□

[16] The proof in [23] uses quantum phase estimation on $(\partial \pm \partial^\dagger)$ with respect to the witness state to check whether it is a state with low eigenvalue to within polynomial accuracy in polynomial time.

Chapter 2

Supplementary Discussion

2.1 Simplicial Complexes as SUSY many-body systems

We have shown that the complexity of the homology problem, a canonical problem in classical topology, is captured by quantum complexity classes. The technical reduction from Section 1.3, however, does not explain *why* this is the case at a deeper level. As already mentioned in the Introduction, the reason underlying this was suggested in [26, 23]. Indeed, as pointed out in these references, there is a deep reason why one should expect the problem of homology to be quantum mechanical, which dates back to the pioneering work of Witten [27]. In this paper Witten considered quantum mechanical systems with supersymmetry, a special class of systems with a symmetry relating bosonic states to fermionic states. It was then shown that states with $E = 0$ in such systems are in 1-to-1 correspondence with elements of homology. Although Witten focused on *continuous* quantum mechanical systems, this relation also holds for discrete quantum mechanical systems of interest here. Here we spell out this relation in detail for the case of general simplicial complexes and discuss the special case of the clique/independence complex.

2.1.1 SUSY quantum mechanics

The Hilbert space $\mathcal{H}$ of *any* quantum mechanical system can be decomposed as $\mathcal{H} = \mathcal{H}_B \oplus \mathcal{H}_F$, where $\mathcal{H}_B$ is the space of bosonic states $|\psi_B\rangle$ and $\mathcal{H}_F$ the space of fermionic states $|\psi_F\rangle$. These are formally distinguished by the action of the "parity operator" $\mathcal{P}$, acting as

$$\mathcal{P}\,|\psi\rangle = \begin{cases} +\,|\psi\rangle & \text{if } |\psi\rangle \in \mathcal{H}_B \\ -\,|\psi\rangle & \text{if } |\psi\rangle \in \mathcal{H}_F \end{cases} \tag{2.1.1}$$

Bosonic and fermionic states correspond to states which are symmetric or antisymmetric under the exchange of particles, respectively.

The parity operator can also be used to define the notion of bosonic and fermionic *operators*. By definition, an operator $\mathcal{O}_B$ is bosonic if it commutes with the parity operator, $[\mathcal{P}, \mathcal{O}_B] = 0$. An operator $\mathcal{O}_F$ is fermionic if it anticommutes with the parity operator, $\{\mathcal{P}, \mathcal{O}_F\} = 0$.

By definition, a quantum mechanical system is supersymmetric if there exists an operator $\mathcal{Q}$ sending bosonic states into fermionic states and vice versa, and squaring to zero:[1]

$$\mathcal{Q} : (\mathcal{H}_B, \mathcal{H}_F) \to (\mathcal{H}_F, \mathcal{H}_B) \qquad\qquad \mathcal{Q}^2 = 0\,. \tag{2.1.2}$$

[1] Technically, this is called an $\mathcal{N} = 2$ SUSY quantum mechanics (see [27] and e.g. [23] for more details). It is one of the simplest

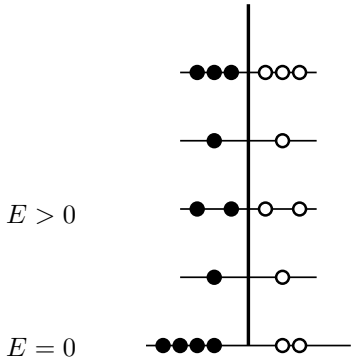

Figure 2.1: The spectrum of supersymmetric quantum mechanics. Black dots represent bosonic states and white ones fermionic states. All states with $E > 0$ come in boson/fermion pairs. Supersymmetric ground states ($E = 0$), if there are any, are not necessarily paired.

The operator $\mathcal{Q}$ is known as the "supercharge" of the system. By consistency of the definitions above the supercharge must anticommute with the parity operator and is thus a fermionic operator. By definition, the Hamiltonian of the system is given by

$$H := \{\mathcal{Q}, \mathcal{Q}^\dagger\} = \mathcal{Q}\mathcal{Q}^\dagger + \mathcal{Q}^\dagger\mathcal{Q}\,. \tag{2.1.3}$$

Note that H sends bosonic states into bosonic states and fermionic states into fermionic states and is therefore a bosonic operator. Note that due to the nilpotency condition

$$[\mathcal{Q}, H] = [\mathcal{Q}^\dagger, H] = 0 \tag{2.1.4}$$

and thus $\mathcal{Q}$ and $\mathcal{Q}^\dagger$ are symmetries of the system. They are not traditional symmetries since they are generated by *fermionic* operators, rather than the more standard symmetries such as translational or rotational symmetry which are generated by bosonic operators.

A few remarkable properties of supersymmetric Hamiltonians follow directly from the definitions above. The first, is that the Hamiltonian is positive semidefinite:

$$\langle\psi|\, H\,|\psi\rangle = \langle\psi|\,(\mathcal{Q}\mathcal{Q}^\dagger + \mathcal{Q}^\dagger\mathcal{Q})\,|\psi\rangle = |\mathcal{Q}\,|\psi\rangle|^2 \big|\mathcal{Q}^\dagger\,|\psi\rangle\big|^2 \geq 0\,. \tag{2.1.5}$$

Thus, the lowest possible energy is $E = 0$. Given a particular supersymmetric system, an important question is whether the ground state of the system has $E = 0$ or $E > 0$. If the ground state energy is positive, the system is said to break supersymmetry "spontaneously." It is in general a difficult question to determine whether a SUSY systems preserves or breaks supersymmetry. Note that a state $|\Omega\rangle$ has $E = 0$ if and if

$$E = 0: \qquad \mathcal{Q}\,|\Omega\rangle = \mathcal{Q}^\dagger\,|\Omega\rangle = 0\,. \tag{2.1.6}$$

Such states, if they exist are called SUSY ground states.

Consider states with $E > 0$. Then, it is easy to see that for every bosonic state with energy E, there is a corresponding fermionic state with the same energy. Indeed, let $H\,|\psi_B\rangle = E\,|\psi_B\rangle$, then clearly one of $Q\,|\psi_B\rangle$ and $Q^\dagger\,|\psi_B\rangle$ is non-zero, and by eq. (2.1.4) will have the same energy, E.

examples of supersymmetry, which can also be defined in the context of quantum field theories and (quantum) gravity. A deeper way to understand supersymmetry in these more general contexts is by formulating it as a fermionic symmetry of spacetime.

2.1.2 Simplicial complexes as SUSY many-body systems

Consider a simplicial complex K with $n+1$ vertices. Recall an oriented p-simplex is an ordered $(p+1)$-subset of the vertices, $\sigma^{(p)} = [x_0, x_1, \cdots, x_p]$. One may want to denote such a simplex as the n-dimensional array $(z_0, z_1, \cdots, z_n)$, where each $z_i \in \{0, 1\}$ indicates if the 0-simplex $[x_i]$ is not present or present in $\sigma^{(p)}$, respectively, and $\sum_{i=0}^{n} z_i = p+1$. However, this representation does not carry information about the orientation of the original simplex. To remedy this we instead identify simplices with states in the Fock space of $n+1$ fermions, as

$$\sigma^{(p)} \leftrightarrow (a_0^\dagger)^{z_0}(a_1^\dagger)^{z_1} \cdots (a_n^\dagger)^{z_n} |0\rangle \tag{2.1.7}$$

where $|0\rangle$ is the state with no fermions and the operators a_i and their conjugates $a_i^\dagger$ are the standard set of operators satisfying the anticommutation relations

$$\{a_i, a_j^\dagger\} = \delta_{ij}\,, \qquad \{a_i, a_j\} = \{a_i^\dagger, a_j^\dagger\} = 0\,. \tag{2.1.8}$$

Permuting the vertices the LHS of (2.1.7) is correctly accounted for by the exchange of the anticommuting operators on the RHS. The fermion number operator is given by $F = \sum_{i=0}^{n} a_i^\dagger a_i$. The annihilation operators a_i decrease the fermion number by 1 and the creation operators $a_i^\dagger$ increase it by 1. Note that the states in (2.1.7) have $F = \sum_{i=0}^{n} z_i = p+1$. A p-simplex is then identified with a state with fermion number $F = p+1$.

The simplicial boundary operator (1.1.6) is represented very easily in fermionic Fock space:

$$\partial = \sum_{i=0}^{n} a_i\,. \tag{2.1.9}$$

The signs appearing in (1.1.6) are automatically accounted for by the anticommuting nature of the fermionic operators as well as $\partial^2 = \sum_{i<j}\{a_i, a_j\} = 0$. It would be tempting to identify $\partial^\dagger$ with $\sum_{i=0}^{n} a_i^\dagger$ but this would not be generally correct, as some $a_i^\dagger$ may create simplex not in K. We thus define

$$\hat{\partial} = P\partial P\,, \qquad \hat{\partial}^\dagger = P\partial^\dagger P\,, \tag{2.1.10}$$

where P is the projector onto elements in K, which we assume commutes with the fermion number operator $[F, P] = 0$ so that $\hat{\partial} : C_p \to C_{p-1}$ and $(\hat{\partial})^2 = (\hat{\partial}^\dagger)^2 = 0$.[2] The supercharges are then identified as[3]

$$Q = P\partial^\dagger P\,, \qquad Q^\dagger = P\partial P\,, \tag{2.1.11}$$

and the SUSY Hamiltonian is

$$H = \sum_{i,j} P a_i^\dagger P\; a_j P + P a_i P a_j^\dagger P\,. \tag{2.1.12}$$

Note that the locality of H depends on the projectors P. Although these are diagonal in the computational basis they could generically be non-local in the fermionic modes. Let $\mathcal{H}_{E=0}$ be the SUSY groundspace of the system. Since the Hilbert space is graded by the fermion number one has

$$\mathcal{H}_{E=0} = \bigoplus_p \mathcal{H}_{E=0}^{(p)}\,. \tag{2.1.13}$$

[2]The projectors P are strictly speaking not required in ∂ as long as the operator is acting on the space of allowed simplices, as the boundary of a simplex is always contained in the simplicial complex. However, we include these so that ∂ and $\partial^\dagger$ are manifestly Hermitian conjugates of each other.

[3]It is customary to define the supercharge as having fermion number $+1$ and its Hermitian conjugate -1, consistent with the identification below, but the choice $Q = \partial$ would be equally valid.

where $\mathcal{H}^{(p)}_{E=0}$ are the subspaces with fixed fermion number $F = p$. Each subspace is in 1-to-1 correspondence with the reduced homology groups

$$\mathcal{H}^{(p)}_{E=0} \cong \tilde{H}_{p-1}(K, \mathbb{C}) \,, \tag{2.1.14}$$

where we have set $\mathbb{F} = \mathbb{C}$ as general elements in the Hilbert space will have complex coefficients. We illustrate this in the case of the independence complex next.

2.1.3 Independence homology and the fermion hard-core model

As discussed, the independence complex is a particular class of simplicial complexes specified by a graph G. The corresponding many-body systems models are known as the fermion hard-core model introduced in [28]. The Hilbert space is given by all configurations of fermions on a graph G subject to the condition that no two fermions can occupy neighboring vertices (the hard-core condition). The Hilbert space therefore corresponds to the independent sets of G. The supercharges are given by

$$Q = \sum_i P_i a_i^\dagger \,, \qquad Q^\dagger = \sum_i \bar{a}_i P_i \,, \qquad P_i = \prod_{j|(i,j)\in E} (1 - \hat{n}_j) \,, \tag{2.1.15}$$

where $\hat{n}_i = a_i^\dagger a_i$ and the P_i ensure that the operators act within the space of independent sets. These are a special case of the supercharges in eq. (2.1.11), where one uses the fact that for this class of models we have $a_i P = P_i a_i$.

By some simple manipulations the Hamiltonian can be brought into the form

$$H = \sum_{(i,j)\in E} P_i a_i^\dagger a_j P_j + \sum_{i\in V} P_i \,. \tag{2.1.16}$$

Since the Hilbert space of the theory is spanned by independent sets of G and the supercharge $Q^\dagger$ acts on this space as the boundary operator ∂, the space of supersymmetric ground states is isomorphic to the homology of the independence complex, as observed in [29, 30]. This relation has been used in a number of beautiful works both in the condensed matter physics literature [31, 32, 32–35] as well in the math literature [36–44], in many cases leading to exact determination of the SUSY groundspace for simple graphs G, such as the square or other regular lattices. The results of subsection 1.3.2, however, indicate that there can be no efficient algorithm to determine the groundspace of the fermion hard-core model on a generic graph G (even when restricted to graphs of constant degree – see subsection 1.3.3.

Let us illustrate this explicitly for the graphs constructed in the reduction of subsection 1.3.2. Consider a single triangle G_1. Due to the hard-core condition, at most one fermion can occupy the triangle and the Hilbert space is spanned by the four states:

$$|b\rangle = |000\rangle \,, \qquad |f_1\rangle = |100\rangle \,, \qquad |f_2\rangle = |010\rangle \,, \qquad |f_3\rangle = |001\rangle \,, \tag{2.1.17}$$

where $|b\rangle$ is a bosonic state with no fermions and the $|f_i\rangle$ are three fermionic states, with a fermion at site $i = 0, 1, 2$. The supercharge is given by

$$Q_1 = \sum_{i=0}^{2} a_i^\dagger P_i \,. \tag{2.1.18}$$

Note that the vacuum state $|b\rangle$ cannot be a supersymmetric ground state since acting with the supercharge gives $Q_1 |b\rangle = |f_0\rangle + |f_1\rangle + |f_2\rangle =: |f\rangle \neq 0$ and thus $(|b\rangle, |f\rangle)$ form a supersymmetric doublet. Indeed, one can easily calculate that the energy of the multiplet is $E = 1$. This leaves two fermionic states unpaired, which must therefore have $E = 0$ and span a two-dimensional SUSY groundspace. These correspond to the two non-trivial homology classes outlined in subsection 1.3.1.

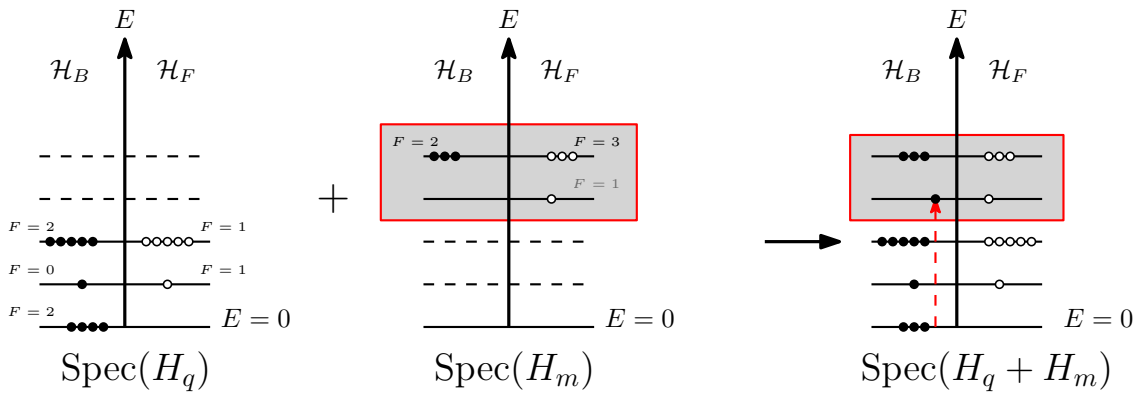

Figure 2.2: Lifting a single SUSY ground state by introducing a mediator vertex connecting to two triangles as in eq. (2.1.20). H_q is a supersymmetric Hamiltonian, so all non-zero eigenavlues are paired up. The Hamiltonian H_m is not supersymmetric, and includes unpaired non-zero eigenvalues. When the two Hamiltonians are added together an unpaired eigenvalue from H_m can pair up with a zero eigenvalue from H_q, lifting one state from the SUSY groundspace, as desired.

Consider now two triangles G_2 and supercharge $Q_2 = \sum_{i=0}^{5} a_i^\dagger P_i$. The system has a total of $1+6+9$ states with $F = 0, 1, 2$, respectively and two SUSY ground states at $F = 2$. Now, consider adding a mediator vertex m with a staggering parameter λ_m. The introduction of the new vertex incorporates $9 = 1+4+4$ new states with $F = 1, 2, 3$, respectively, into the Hilbert space. The supercharge is given by

$$Q = Q_2 + Q_m \,, \tag{2.1.19}$$

where $Q_m = a_m^\dagger P_m$ and the full Hamiltonian is now given by:

$$H = H_q + H_m \tag{2.1.20}$$

where

$$H_q = \{Q_2, Q_2^\dagger\} \,, \qquad H_m = \{Q_2, Q_m^\dagger\} + \{Q_m, Q_2^\dagger\} + \{Q_m, Q_m^\dagger\} \tag{2.1.21}$$

The first term in eq. (2.1.20) is the (manifestly supersymmetric) Hamiltonian corresponding to the triangles with no mediators present. Therefore, as outlined above, all of its eigenvalues are either zero, or come in supersymmetric pairs. The additional term H_m by itself does not correspond to a supersymmetric Hamiltonian. Therefore it can have unpaired non-zero eigenvalues. When adding the two Hamiltonians together the resultant Hamiltonian is non-zero. In order to lift one of the zero eigenvalues of H_q to a non-zero eigenvalue it needs to pair up, and it can do this because H_m has unpaired non-zero eigenvalues (see Fig. 2.2 for an illustration).

Now consider n disconnected triangles G_n. The full system is in a SUSY ground state only if each triangle is in a SUSY ground state and thus the only SUSY ground states are found at $F = n$ and there are 2^n of them, consistent with

$$\tilde{H}_{n-1}(\Sigma_n) = (\mathbb{C}^2)^{\otimes n} \,. \tag{2.1.22}$$

In order to implement the projectors needed for H_{Bravyi} we introduce mediator vertices to mediate interactions between the triangles. Certain states then acquire a non-zero energy and are thus pushed out of the SUSY groundspace.

Note we do not claim that the quantum k-SAT Hamiltonian $H = \sum_a \Pi_a$ can be interpreted as a supersymemtric Hamiltonian, only that there is a supersymmetric Hamiltonian with the same dimensional ground space. The excited spectrum will generically be different.

Bibliography

[1] B. R. Donald and D. R. Chang, "On computing the homology type of a triangulation," 1990.

[2] V. Kaibel and M. E. Pfetsch, "Some Algorithmic Problems in Polytope Theory," *arXiv Mathematics e-prints* (Feb., 2002) math/0202204, arXiv:math/0202204 [math.CO].

[3] P. O. de Mendez, "Geometric realization of simplicial complexes," in *Graph Drawing*, J. Kratochvíyl, ed., pp. 323–332. Springer Berlin Heidelberg, Berlin, Heidelberg, 1999.

[4] A. Hatcher, C. U. Press, and C. U. D. of Mathematics, *Algebraic Topology*. Algebraic Topology. Cambridge University Press, 2002. https://books.google.com/books?id=BjKs86kosqgC.

[5] G. Petri, P. Expert, F. Turkheimer, R. Carhart-Harris, D. Nutt, P. J. Hellyer, and F. Vaccarino, "Homological scaffolds of brain functional networks," *Journal of The Royal Society Interface* **11** (2014) no. 101, 20140873.

[6] C. Giusti, R. Ghrist, and D. S. Bassett, "Two's company, three (or more) is a simplex," *Journal of computational neuroscience* **41** (2016) no. 1, 1–14.

[7] M. Reimann, M. Nolte, M. Scolamiero, K. Turner, R. Perin, G. Chindemi, P. Dlotko, R. Levi, K. Hess, and H. Markram, "Cliques of Neurons Bound into Cavities Provide a Missing Link between Structure and Function," *Frontiers in Computational Neuroscience* **11** (June, 2017) 1–16. https://hal.archives-ouvertes.fr/hal-01706964.

[8] S. Bravyi, "Efficient algorithm for a quantum analogue of 2-SAT," *Contemporary Mathematics* **536** (2011) 33–48, arXiv:quant-ph/0602108.

[9] D. Gosset and D. Nagaj, "Quantum 3-sat is QMA_1-complete," *2013 IEEE 54th Annual Symposium on Foundations of Computer Science* (Oct, 2013) . http://dx.doi.org/10.1109/FOCS.2013.86. arXiv:1302.0290.

[10] L. M. Adleman, J. DeMarrais, and M.-D. A. Huang, "Quantum computability," *SIAM Journal on Computing* **26** (1997) no. 5, 1524–1540, https://doi.org/10.1137/S0097539795293639. https://doi.org/10.1137/S0097539795293639.

[11] Y. Shi, "Both toffoli and controlled-not need little help to do universal quantum computing," *Quantum Information & Computation* **3** (2003) no. 1, 84–92.

[12] S. Aaronson, "On perfect completeness for qma," 2008.

[13] S. P. Jordan, H. Kobayashi, D. Nagaj, and H. Nishimura, "Achieving perfect completeness in classical-witness quantum merlin-arthur proof systems," 2012.

[14] B. Fefferman and C. Y.-Y. Lin, "A complete characterization of unitary quantum space," 2016.

[15] A Mathematica file containing details of calculations is available at:. https://www.dropbox.com/sh/1zfnqkmi94lxvm2/AAD0oquHvE5riSBa0Vje_wKWa?dl=0.

[16] M. Adamaszek and J. Stacho, "Complexity of simplicial homology and independence complexes of chordal graphs," *Computational Geometry* **57** (2016) 8–18.

https://www.sciencedirect.com/science/article/pii/S0925772116300463.

[17] A. Schmidhuber and S. Lloyd, "Complexity-theoretic limitations on quantum algorithms for topological data analysis," 2022.

[18] S. Lloyd, S. Garnerone, and P. Zanardi, "Quantum algorithms for topological and geometric analysis of data," *Nature communications* **7** (2016) no. 1, 1–7.

[19] C. Reiher, "The clique density theorem,"*Annals of Mathematics* **184** (nov, 2016) 683–707. https://doi.org/10.4007%2Fannals.2016.184.3.1.

[20] J. Watrous, "Succinct quantum proofs for properties of finite groups," 2000. https://arxiv.org/abs/cs/0009002.

[21] J. Watrous, "Quantum computational complexity," 2008. https://arxiv.org/abs/0804.3401.

[22] D. Horak and J. Jost, "Spectra of combinatorial laplace operators on simplicial complexes," *Advances in Mathematics* **244** (2013) 303–336. https://www.sciencedirect.com/science/article/pii/S0001870813001722.

[23] C. Cade and P. M. Crichigno, "Complexity of Supersymmetric Systems and the Cohomology Problem," arXiv:2107.00011 [quant-ph].

[24] C. Gyurik, C. Cade, and V. Dunjko, "Towards quantum advantage via topological data analysis," 2020. https://arxiv.org/abs/2005.02607.

[25] B. Brown, S. T. Flammia, and N. Schuch, "Computational difficulty of computing the density of states,"*Physical Review Letters* **107** (jul, 2011) . https://doi.org/10.1103%2Fphysrevlett.107.040501.

[26] P. M. Crichigno, "Supersymmetry and Quantum Computation," arXiv:2011.01239 [quant-ph].

[27] E. Witten, "Supersymmetry and Morse theory," *J. Diff. Geom.* **17** (1982) no. 4, 661–692.

[28] P. Fendley, K. Schoutens, and J. de Boer, "Lattice models with $\mathcal{N} = 2$ supersymmetry,"*Physical Review Letters* **90** (Mar, 2003) . http://dx.doi.org/10.1103/PhysRevLett.90.120402.

[29] J. Jonsson, "Certain homology cycles of the independence complex of grids," *Discrete & Computational Geometry* **43** (2010) no. 4, 927–950. https://doi.org/10.1007/s00454-009-9224-9.

[30] L. Huijse and K. Schoutens, "Superfrustration of charge degrees of freedom," *The European Physical Journal B* **64** (2008) no. 3, 543–550. https://doi.org/10.1140/epjb/e2008-00150-9.

[31] M. Beccaria and G. F. De Angelis, "Exact ground state and finite-size scaling in a supersymmetric lattice model," *Physical review letters* **94** (2005) no. 10, 100401.

[32] P. Fendley, K. Schoutens, and J. de Boer, "Lattice models with n= 2 supersymmetry," *Physical review letters* **90** (2003) no. 12, 120402.

[33] P. Fendley and K. Schoutens, "Exact results for strongly correlated fermions in 2+ 1 dimensions," *Physical review letters* **95** (2005) no. 4, 046403.

[34] L. Huijse and K. Schoutens, "Superfrustration of charge degrees of freedom," *The European Physical Journal B* **64** (2008) no. 3, 543–550.

[35] L. Huijse, J. Halverson, P. Fendley, and K. Schoutens, "Charge frustration and quantum criticality for strongly correlated fermions," *Physical review letters* **101** (2008) no. 14, 146406.

[36] M. Adamaszek, "Special cycles in independence complexes and superfrustration in some lattices," *Topology and its Applications* **160** (2013) no. 7, 943–950.

[37] L. Huijse and K. Schoutens, "Supersymmetry, lattice fermions, independence complexes and cohomology theory," *Advances in Theoretical and Mathematical Physics* **14** (2010) no. 2, 643–694.

[38] J. Jonsson, "Hard squares with negative activity on cylinders with odd circumference," *the electronic journal of combinatorics* (2009) R5–R5.

[39] J. Jonsson, "Hard squares on grids with diagonal boundary conditions," *preprint* (2006) .

[40] R. Baxter, "Hard squares for z=–1," *Annals of Combinatorics* **15** (2011) no. 2, 185–195.

[41] M. Bousquet-Mélou, S. Linusson, and E. Nevo, "On the independence complex of square grids," *Journal of Algebraic combinatorics* **27** (2008) no. 4, 423–450.

[42] A. Engström, "Upper bounds on the witten index for supersymmetric lattice models by discrete morse theory," *European Journal of Combinatorics* **30** (2009) no. 2, 429–438.

[43] P. Fendley, K. Schoutens, and H. van Eerten, "Hard squares with negative activity," *Journal of Physics A: Mathematical and General* **38** (2004) no. 2, 315.

[44] P. Csorba, "Subdivision yields alexander duality on independence complexes," *the electronic journal of combinatorics* (2009) R11–R11.

[45] A. Y. Kitaev, A. Shen, and M. N. Vyalyi, "Classical and quantum computing," in *Quantum Information*, pp. 203–217. Springer New York, New York, NY, 2002. `http://link.springer.com/chapter/10.1007/978-0-387-36944-0{_}13http://link.springer.com/10.1007/978-0-387-36944-0{_}13`.

[46] D. Aharonov, W. van Dam, J. Kempe, Z. Landau, S. Lloyd, and O. Regev, "Adiabatic quantum computation is equivalent to standard quantum computation,". `https://arxiv.org/abs/quant-ph/0405098`.

[47] R. Oliveira and B. M. Terhal, "The complexity of quantum spin systems on a two-dimensional square lattice,". `https://arxiv.org/abs/quant-ph/0504050`.

[48] L. Zhou and D. Aharonov, "Strongly universal hamiltonian simulators," 2021. `https://arxiv.org/abs/2102.02991`.